Coordination Chemistry Reviews 437 (2021) 213757

Contents lists available at ScienceDirect

Coordination Chemistry Reviews

journal homepage: www.elsevier.com/locate/ccr

Review

# Tuning photoactive metal–organic frameworks for luminescence and photocatalytic applications

Éadaoin Whelan [a,*], Friedrich W. Steuber [a], Thorfinnur Gunnlaugsson [a,b], Wolfgang Schmitt [a,*]

[a] School of Chemistry and SFI AMBER & SSPC Research Centres, University of Dublin, Trinity College, Dublin 2, Ireland
[b] Trinity Biomedical Sciences Institute (TBSI), University of Dublin, Trinity College, Dublin 2, Ireland

ARTICLE INFO

*Article history:*
Received 13 October 2020
Received in revised form 27 November 2020
Accepted 16 December 2020
Available online 12 March 2021

*Keywords:*
Metal-organic Frameworks
Porous materials
Photoactive materials
Luminescence
Sensing
Photocatalysis

ABSTRACT

Metal-organic frameworks (MOFs) are a class of porous materials, constructed from organic and inorganic components. MOFs have been explored for a diverse range of applications due to their tunable structures, porosities, and properties. This review highlights examples of the applications of photoactive MOFs, with a focus on the effect of MOF components, such as organic linkers, inorganic units and framework guests, on the optical and electronic properties of the materials. Developments in utilising luminescent MOFs as chemical sensors and as light emitting materials are discussed, in addition to recent advances in designing MOF-based photocatalysts for water splitting, $CO_2$ reduction and organic reactions.


**Contents**



* Corresponding authors.
*E-mail addresses:* nifhaole@tcd.ie (É. Whelan), schmittw@tcd.ie (W. Schmitt).

https://doi.org/10.1016/j.ccr.2020.213757
0010-8545/

## 1. Introduction

Metal-organic frameworks (MOFs), or related porous coordination polymers (PCPs) can be regarded as a class of porous crystalline materials, which self-assemble from organic linkers and individual metal ions or coordination cluster nodes.[1,2] The organic linkers are multidentate species, which bridge metal ions or cluster moieties to form extended two- or three-dimensional structures. Early pioneering work demonstrated that through variation of the components used to construct MOFs, a wide range of structures were accessible.[3–9] Research into the control of the architecture of MOFs led to the development of reticular chemistry and related topological concepts.[10]

Reticular chemistry concepts are based on the realisation that a MOF can be reduced to the geometrical features of its subcomponents and categorised accordingly.[10] The inorganic node of the structure determines the relative orientation in which the organic linkers assemble. The organic linkers serve as geometrically defined connectors between the inorganic subunits. Both organic and inorganic components are often classified as secondary building units (SBUs), in analogy to zeolite topochemistry:[11,12] Reticular synthetic approaches take advantage of the specific geometries and chemical amiability of SBUs, producing extended network structures whose topologies relate to those of purely inorganic '*default*' structures. A key principle that governs the synthesis of MOFs stems from the realisation that MOFs whose components possess the same geometrical features form isoreticular structures that adopt analogous topologies, or the same nets.[13]

As reticular chemistry and related synthetic concepts gained increasing importance, and their applications resulted in the discovery of prodigious numbers of new structures, universal nomenclatures for structure classification and identification were developed, for instance through collaborative efforts between Blatov, O'Keeffe and Proserpio.[14] The Reticular Chemistry Structure Resource (RCSR) database categorises the structures according to their topologies[15]; the RCSR symbols are composed of three lower case bold letters with abbreviations either based on materials with that topology (e.g. **dia** for diamond or **pto** for platinum oxide) or geometrical shapes (e.g. **pcu** for primitive cubic lattice or **sql** for square lattice, etc.).

In addition to their tunable structures and pore volumes,[16,17] MOFs and related metal–organic materials offer an advantage over other conventional inorganic porous materials, such as zeolites, as their properties can be tuned for specific applications by varying the nature of the linkers and the metal ions in the structure.[18–20] Additionally, the porosity of MOFs allows incorporation of various guest molecules into their voids, which can influence the properties of the materials.[21] The chemical and structural versatility of MOFs, as well as their potentially high surface areas and porosity, have facilitated their application as catalysts,[22–24] materials for gas storage[25] and separation,[26,27] as chemical sensors,[28,29] as photosensitisers for photodynamic therapy[30] and other applications.[31]

The ability to incorporate photosensitising ligands (e.g. organic chromophores, polyaromatic coordinating ligands, suitable coordination complexes, etc.) into MOFs has led to their development as light-harvesting materials.[22,32] Significant research activities have been carried out to investigate how the choice of the organic linker and inorganic node used in the construction of MOFs, as well as interactions with guest molecules, allow their photochemical properties to be controlled.[33] Hence, by systematic variation of the individual MOF components, the light absorption characteristics, as well as the luminescence output can be tuned towards specific wavelengths.[34] Additionally, MOFs can be tailored towards photocatalytic applications by incorporation of the appropriate components or functional groups.[35–37]

Herein, the design principles of photoactive MOFs are highlighted, in the context of two key aspects. A primary section discusses the application of *MOFs as photoluminescent materials*, for example, as light emitting materials with tunable emission characteristics, and as chemical sensors with luminescence responses. The second aspect explores the design of *MOFs as photocatalysts* for energy-conversion reactions such as water splitting, $CO_2$ reduction or for light-driven organic reactions, such as degradation of organic pollutants. Particular attention is given to how the choice of the constitutional components of MOFs influences the photoactivity of these materials. This article is not intended to be a definitive comprehensive review of the current state-of-the-art within this fast developing field of research, however, it will explore some selected examples of recent advancements in areas which may provide inspiration for those new to the research field. Organic linkers of the individual MOFs that are discussed, and their abbreviations are shown in Fig. 1.

## 2. Photochemistry of MOFs

### 2.1. Absorption of light by MOFs

The design and synthesis of a photoactive MOF requires the incorporation of a light-harvesting unit into the structure. Typically, this is achieved by using an appropriate organic linker in the MOF structure, though light-harvesting guests can also be incorporated into the voids of the porous framework.[38] In some rarer cases, direct excitation of metal ions or metal clusters is also possible, for example, in $Fe^{III}$-based MOFs containing $\{Fe^{III}_3(\mu_3\text{-}O)\}^{7+}$ clusters.[39] By varying the organic linker, MOFs can be designed to absorb light in specific regions of the UV–visible spectrum.[40]

Many MOFs utilise aromatic organic linkers, which absorb light in either the UV or visible region of the spectrum.[41,42] Excitation of these organic linkers leads to n-$\pi^*$- or $\pi$-$\pi^*$-based transitions. The range of wavelengths in which these compounds absorb light can be varied by extending the conjugated aromatic system of the linker, or incorporating various functional groups on the backbone structure of the linker.[43,44] Alternatively, metalloligands can be employed as photosensitisers in MOFs. Of note are MOFs composed of metalloporphyrin ligands, which show great promise as photoactive materials, due to their ability to absorb visible light across a broad region of the spectrum. The photocatalytic properties of metalloporphyrin-based MOFs can be varied by changing the metal ion within the porphyrin cavity. For example, metallation of porphyrin linkers with high valent metal ions such as $In^{III}$ and $Sn^{IV}$ gives MOFs with oxidative photoexcited states that can facilitate organic reactions, for example, the Mannich reaction, aerobic amine coupling, and hydroxylation of arylboronic acids.[45] Thus, porphyrinic MOFs are being explored as promising and versatile photocatalytic materials.[46,47]

Furthermore, the use of polypyridyl ligands that can facilitate ligand-centred, metal-to-ligand and ligand-to-metal-based transitions can be used in the generation of photosensitisers in MOFs. MOFs based on $Ru^{II}$ or $Ir^{III}$ photosensitisers, which are well known as excellent photo-cleavage agents for nucleic acids such as DNA, [48,49] have been widely reported in recent times.[50,51] $Ru^{II}$ polypyridyl-based photosensitisers offer advantages as linkers due to their ability to harvest visible light,[52] their long-lived excited states, and their ability to undergo photoinduced redox reactions.[53] Metalloligands employing earth-abundant metal ions have also been incorporated into MOF structures as photosensitisers, for example those based on $Cu^{I}$ species.[54,55]

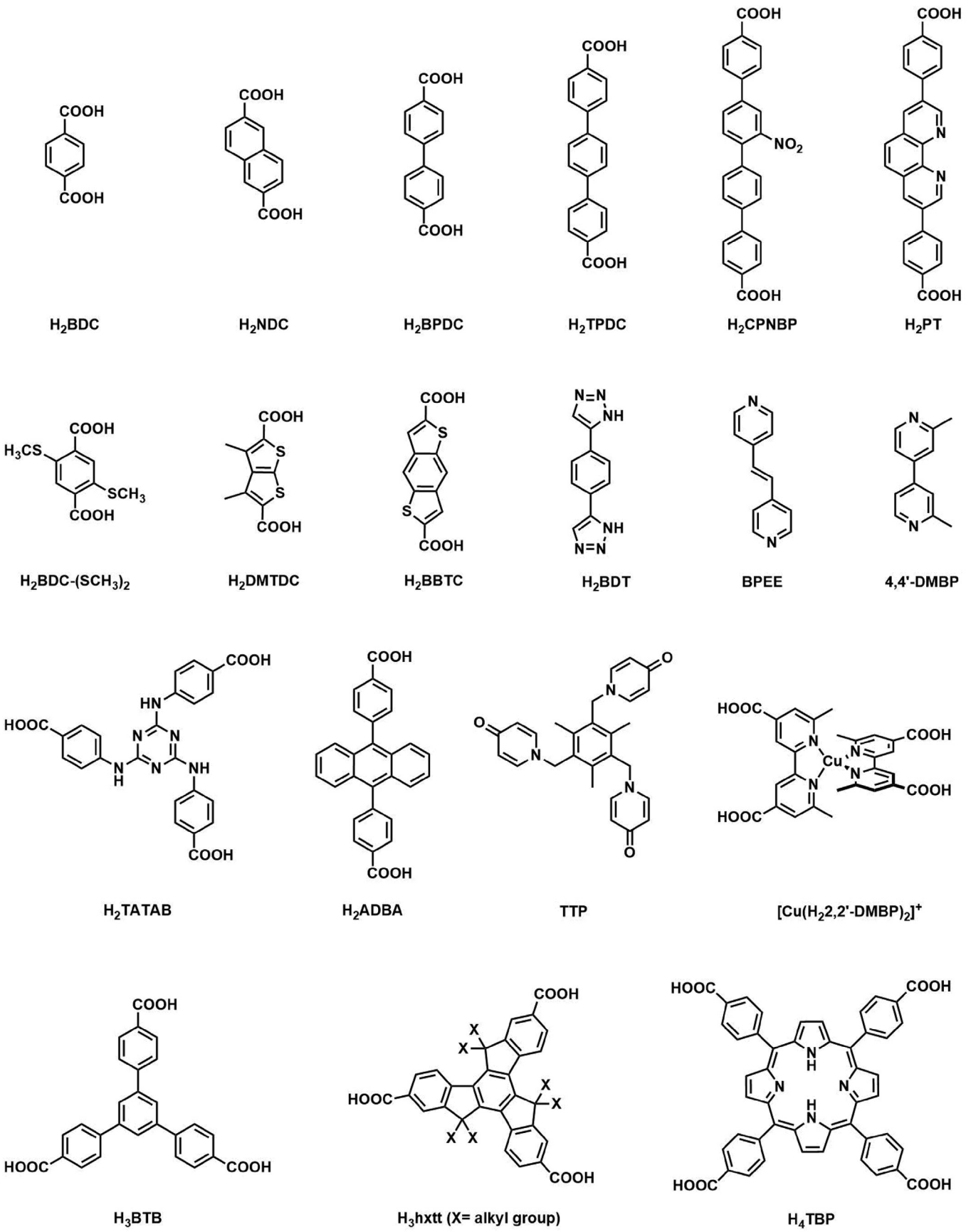


**Fig. 1.** A small selection of organic linkers used in the construction of photoactive MOFs, and corresponding abbreviations as they appear in this article.

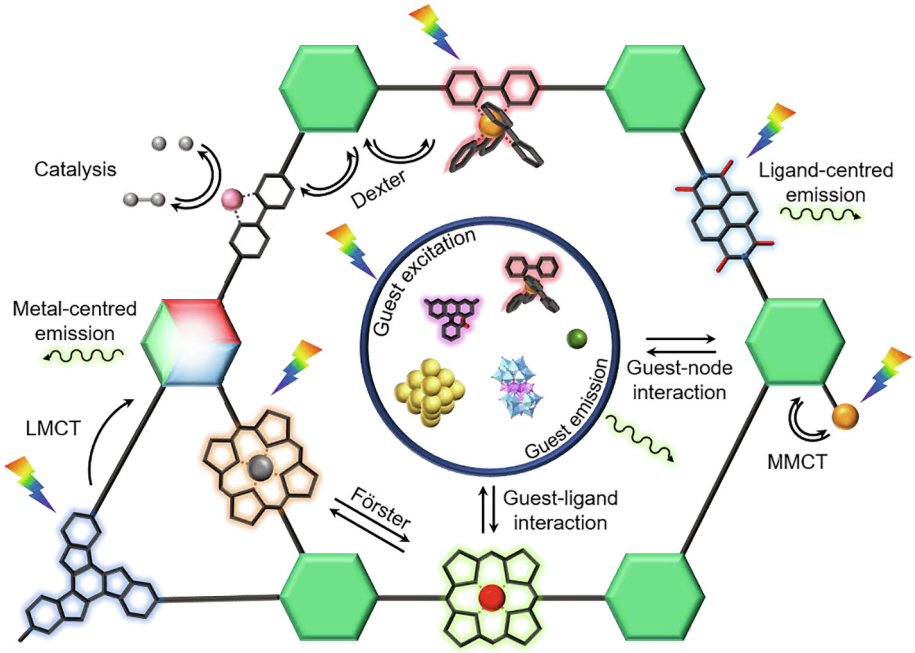


**Fig. 2.** Schematic representation of the absorption and emission processes in photoactive MOFs, showing examples of photoactive organic linkers and inorganic nodes are represented by hexagons. Polyoxometalate (POM) structure produced from Ref. [60].

The diversity of ligands that can be used in the construction of MOFs can allow for further tuning of the optical band gaps of these materials. For example, by functionalisation of the ligand used in a MOF denoted as MIL-125 (MIL = Matériaux de l'Institut Lavoisier), the optical band gap of this material could be varied.[56] MIL-125 consists of 1,4-benzenedicarboxylate ($BDC^{2-}$) linkers that bridge octanuclear cyclic Ti-oxo clusters. Walsh and co-workers reported that the introduction of amine functional groups onto the $BDC^{2-}$ linker of MIL-125 led to a shift of the absorption onset of these MOFs from the UV region to the visible region of the electromagnetic spectrum. Furthermore, functional groups which impart weaker electron donating effects than amines revealed a reduced influence on the band gap, with smaller shifts observed for -Cl, $-CH_3$, and –OH substituents.

### 2.2. Luminescence processes of MOFs

Luminescence is defined as emission of light from a substance, which occurs following absorption of radiative energy, either directly or via sensitisation processes involving energy or electron transfer processes.[57] Two categories of luminescence exist, fluorescence and phosphorescence. Fluorescence occurs without a change in spin, when light is emitted from singlet excited states and fluorescence lifetimes are short, in the region of $10^{-12}$ to $10^{-6}$ s.[58] In contrast, phosphorescence occurs when spin-forbidden transitions occur resulting in the emission of a photon, for example, from triplet excited states to singlet ground-states. Phosphorescence lifetimes are longer than those observed for fluorescence processes, with typical values varying between $10^{-6}$ and $10^{2}$ s.[58] While not common for organic ligands (except at low temperatures), phosphorescence can be facilitated through intersystem crossing by the so-called heavy atom effect that is characteristic for many d- and f-block metal complexes (e.g. $Ru^{II}$ polypyridyl complexes which normally emit from $^3$MLCT states).

Generally, luminescence occurs following absorption of radiation of a specific wavelength, commonly, X-ray, UV or visible light, and emission of light at a different wavelength. The emitted light is usually lower in energy than the absorbed light, and the difference in energy between the maximum of the absorbed light and the maximum of the emitted light is known as the Stokes shift. Alternatively, upconversion may occur, a phenomenon in which absorption of two or more photons results in the emission of one photon of higher energy.[59] In this case, the energy difference is quantified by the anti-Stokes shift.

Due to the hybrid nature of MOF structures, luminescence in MOFs can arise from multiple different sources, as highlighted in Fig. 2. These include,

- Ligand-centred emission
- Ligand-to-ligand charge transfer (LLCT)
- Ligand-to-metal charge transfer (LMCT)
- Metal-to-ligand charge transfer (MLCT)
- Metal-to-metal charge transfer (MMCT)
- Metal-centred emission
- Interactions with guest molecules.

Combinations of more than one of these effects can also be observed in luminescent MOFs.

Linkers in MOFs are constrained in ordered positions and as a result, the photochemical properties of the linkers differ from those of the free ligand in solution. In the rigid environment of MOFs, non-radiative processes from the linker excited state are less efficient, leading to enhancement of the linker fluorescence.[61–63] Ligand-centred emission is commonly observed in MOFs based on $d^{10}$ metal ions such as $Zn^{II}$ and $Cd^{II}$ systems.[64] Due to their closed shell electron configuration, d-d transitions cannot occur, and the metal ions cannot be readily oxidised or reduced, leading to ligand-centred emission characteristics.

Luminescence can also occur via LMCT and MLCT interactions in MOFs. Charge-transfer luminescence occurs due to a transition from the charge-transfer excited state to the ground state. LMCT excited states occur via transfer of electrons from an orbital centred on a linker, to an orbital of a metal ion. The opposite effect is facilitated by MLCT, which involves electronic transitions from

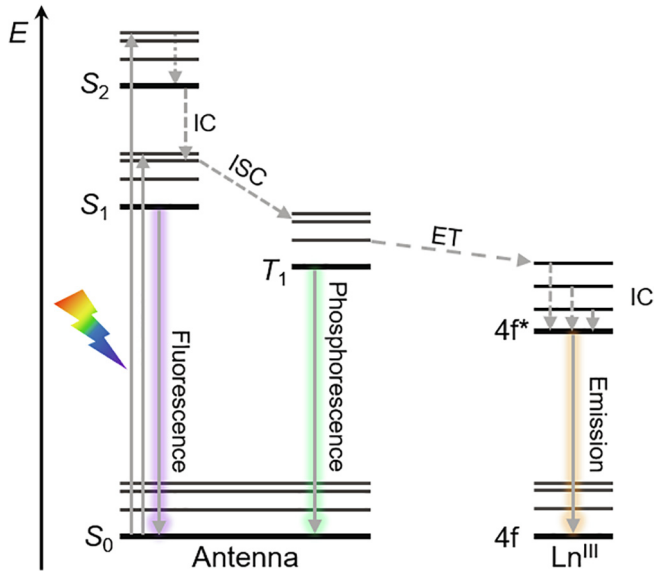


**Fig. 3.** A simplified diagram depicting the antenna effect in a $Ln^{III}$ ion. The solid grey arrows represent absorption of a photon, which can be followed by fluorescence, intersystem crossing (ISC). After ISC occurs, phosphorescence can occur from the triplet excited state of the antenna, or energy transfer can occur, resulting in emission of a photon from the $Ln^{III}$ ion. Internal conversion (IC) can occur as a non-radiative transition between excited states with the same spin.

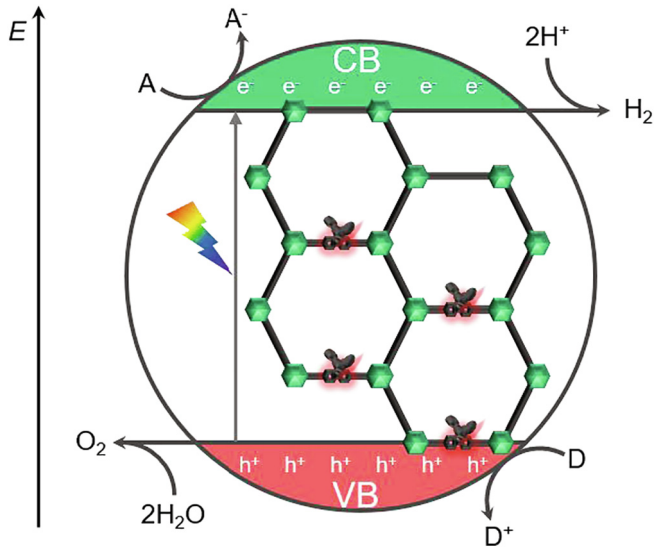


**Fig. 4.** Schematic representation of catalytic reactions after photoinduced charge transfer in a MOF. Excitation of electrons ($e^-$) from the valence band (VB) to the conduction band (CB) results in the formation of holes ($h^+$). Redox reactions can occur by oxidation of an electron donor (D) or reduction of an electron acceptor (A). Furthermore, photo-generated holes can lead to water oxidation, and photoexcited electrons can reduce $H^+$ to $H_2$.

metal orbitals to orbitals of the linkers. MLCT is commonly observed in MOFs containing metal ions in low oxidation states, that can readily be oxidised further.

Metal-centred emissions are typically observed in lanthanide-based MOFs (Ln-MOFs).[65] In these systems the shielding of the 4f orbitals by the $5p^6 6s^2$ shells results in characteristic narrow-line emission, predominantly in the visible and near-infrared regions of the electromagnetic spectrum. The f-f transitions are Laporte forbidden, hence, the absorption coefficients for these transitions are small, typically less than 3 $M^{-1}$ $cm^{-1}$.[66] To excite lanthanide ions effectively, the antenna effect must be employed, in which a ligand coordinated to the $Ln^{III}$ ion acts as a light harvesting chromophore which sensitises the excited state of the lanthanide ion. Absorption of energy by the ligand results in spin-allowed excitation from the ground state to the singlet excited state $S_1$ ($S$ = singlet). Intersystem crossing (ISC) can then occur from the ligand-centred $S_1$ excited state to the triplet excited state, $T_1$ ($T$ = triplet). Energy can then be transferred from the long-lived ligand triplet excited state to the $Ln^{III}$ ion. Emission from the resulting $Ln^{III}$ excited state occurs spontaneously, giving metal-centred luminescence in the absence of back energy transfer to the excited state of the ligand.[67] The latter may either reduce the efficiency of the emission process, or quench it entirely. The $T_1$ to $Ln^{III}$ transfer may be facilitated by good overlap between the linker and metal orbitals, involving a double electron transfer, in line with an exchange or Dexter mechanism. More predominate in coordination compounds is a Förster mechanism, whereby the dipole moments of the 4f orbitals couple the dipole moment of the $T_1$ state. Similarly, dipole–multipole transfers and charge-transfer states can play a role in the sensitisation of $Ln^{III}$ ions. In mixed-metal MOFs composed of transition metal-based linkers and $Ln^{III}$ nodes, sensitisation of the $Ln^{III}$ ions can occur via the $^3$MLCT excited states of the transition metal. Metal-centred emission following sensitisation is also observed in actinide-based MOFs.[68] A simplified diagram for the energy migration pathways applicable to Ln-based MOFs is shown in Fig. 3.

The porous structures of MOFs allow the possibility of introducing luminescent guest molecules into their pores. The crystalline nature of MOFs allows guests in the pores of the material to be characterised in great detail.[69,70] Luminescence can arise from these guest molecules,[71] from both the MOF and the guest molecule separately, or via interactions between these guest molecules and the framework structure.[72] The interactions between the guest molecule and the MOF can occur via weak intermolecular interactions, dipole interactions, or through coordination bonds between the guest and open coordination sites on the framework metal ion.[33]

### 2.3. Photocatalysis

Fossil fuels are the world's primary energy source, accounting for over 80% of global energy consumption.[73] Combustion of fossil fuels results in emission of greenhouse gases, and consequently, the increase of global temperatures.[74] As emissions continue to rise, and fossil fuel reserves are depleted, the need for clean energy sources is increasingly urgent. Solar energy is a renewable and unlimited resource, and much research has focused on harnessing this energy to meet the worlds energy demands in a sustainable way. Designing materials that can use light to carry out reactions such as $H_2O$ splitting or $CO_2$ reduction is vital to provide a sustainable method of producing energy.

Photoactive MOFs have been shown to be promising photocatalysts for energy conversion due to their tunable structures and properties. MOFs can behave as heterogeneous catalysts, and offer an advantage over molecular photocatalysts, as their solid-state nature allows facile separation of catalyst from product, thus lowering the risk of contaminating products with toxic metals used for catalysis.[75] Heterogeneous catalysis also allows the catalyst to be recycled readily. Due to the crystalline nature of MOFs, the active sites are arranged in well-defined spatial sites, and the pores of MOFs can be tuned towards specific dimensions, which offers the potential for substrate selectivity.[76,77] Furthermore, porous MOFs are often characterised by a high number of active sites per volume and high diffusion coefficients, which are attractive properties in catalytic materials.[78]

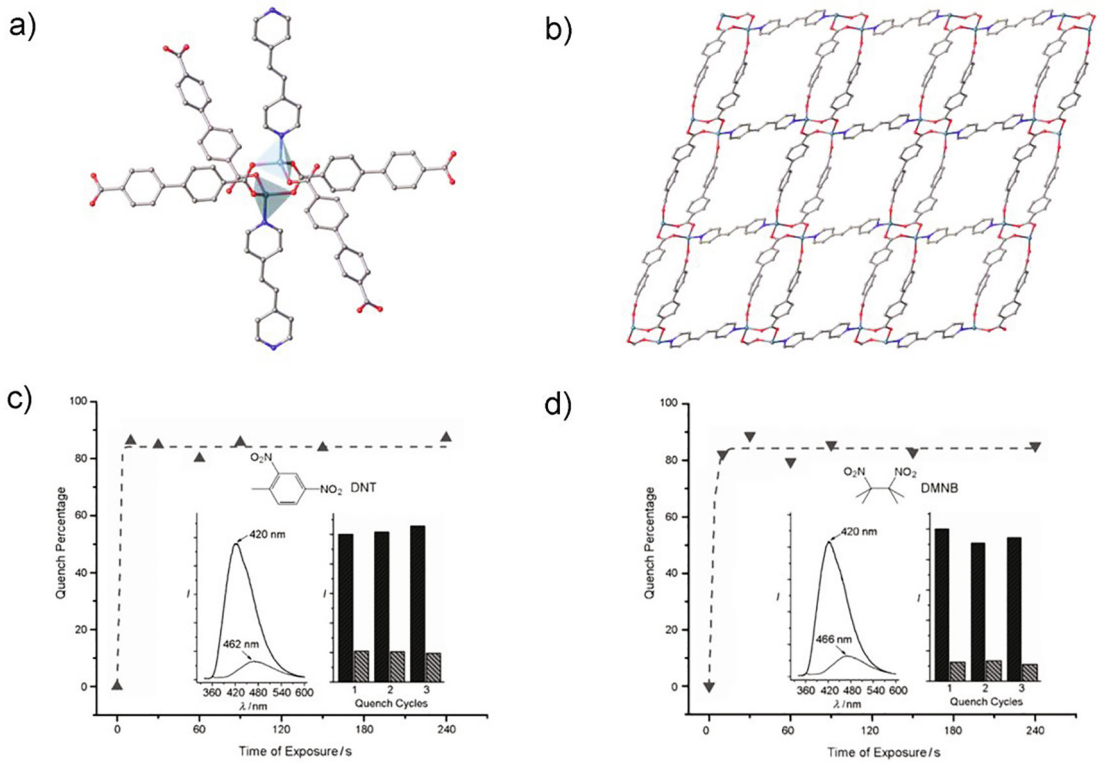


**Fig. 5.** **a)** The coordination environment of the dinuclear $\{Zn_2^{II}\}$ SBU in $[Zn_2(BPDC)_2(BPEE)]$ **b)** View of the structure of $[Zn_2(BPDC)_2(BPEE)]$ (DMF molecules removed for clarity) **c)** and **d)** Time-dependent fluorescence quenching by **c)** DNT and **d)** DMNB. Insets: Fluorescence spectra before and after exposure to vapours of the analytes for 10 s, and emission intensity after three cycles of quenching and regeneration. Reproduced with permission from Ref. [100]. Copyright 2009, Wiley-VCH Verlag GmbH & Co. KGaA, Weinheim.

To function as a photocatalyst, MOFs are required to efficiently separate charges within their structures upon light absorption by a chromophore and promotion of an electron to a higher energy level. This electron can then migrate from the chromophore to a nearby electron acceptor moiety within the structure. The resulting negative charges (electrons) and positive charges (holes) can be used to drive chemical reactions (Fig. 4).[79] Certain requirements are necessary for efficient photocatalysis, such as high molar absorption coefficients, excited state lifetimes that are long enough to allow catalytic conversion to compete with decay of the charge separated state, and finally, suitable redox potentials to drive the desired reactions.[80]

## 3. Utilising MOF luminescence

### 3.1. Sensing

The ability to rapidly detect pollutants at low concentrations is vital to identify environmental risks and curtail pollution. The area of luminescent sensing focusing on small molecules and the *receptor-spacer-fluorophore* principles that govern the sensing process have recently been reviewed.[81] The underlying principles are transferable to MOFs, which offer some distinctive advantages over molecular sensors, associated with their intrinsic attributes including porosity and high surface areas. Luminescent MOFs can be used as sensors for a broad range of analytes, including gases, [82] explosive nitroaromatic compounds (NACs),[83,84] cations, [85,86] anions,[87,88] pesticides,[89] and other organic compounds.[90,91] The luminescence response from MOFs upon detection of analytes can result in luminescence quenching,[92] luminescence enhancing,[93,94] or a change in the colour of light emitted.[95,96] Nanoscale MOFs have even been reported to be capable of pH sensing within living cells.[97]

Several mechanisms for luminescence sensing of analytes have been reported in MOFs. These include linker-analyte ion interaction, collapse of the MOF structure in response to the presence of an analyte, cation exchange between the analyte metal ions and framework metal ions, and competitive absorption of excitation wavelength due to overlap of absorption spectra of the MOF and analyte.[98] The advantage of using MOFs that display sensing through non-destructive mechanisms, such as linker-ion interactions, is that the sensor materials can be readily recycled.[99]

#### 3.1.1. Sensing of organic compounds

The first example of a MOF capable of sensing explosive compounds was reported in 2009.[100] Li and co-workers demonstrated that the luminescent MOF $[Zn_2(BPDC)_2(BPEE)]$ ($BPDC^{2-}$ = 4,4′-biphenyldicarboxylate, BPEE = 1,2-bipyridylethene) (Fig. 5a)) is capable of fast, sensitive and reversible detection of explosive compounds. The structure of $[Zn_2(BPDC)_2(BPEE)]$ features one-dimensional channels which are approximately rectangular in shape (Fig. 5b)). These channels contain DMF solvent molecules which can be removed to give a guest-free MOF. The luminescence quenching response of $[Zn_2(BPDC)_2(BPEE)]$ after solvent removal was tested for two analytes, 2,3-dimethyl-2,3-dinitrobutane (DMNB), a volatile organic compound (VOC) used as a taggant for explosives and 2,4-dinitrotoluene (DNT), a volatile impurity found in 2,4,6trinitrotoluene. Thin layers of $[Zn_2(BPDC)_2(BPEE)]$ show solid-state ligand-based luminescence when irradiated under UV light. This luminescence is quenched in response to DNT and DMNB vapours at concentrations of 0.18 ppm and 2.7 ppm respectively. The luminescence bands are also red-shifted in response to the presence of these analytes (Fig. 5c) and d)). Furthermore, the luminescence of solvent-free $[Zn_2(BPDC)_2(BPEE)]$ could be rapidly recovered after sensing, by heating the layers at 150 °C for one minute. The quenching

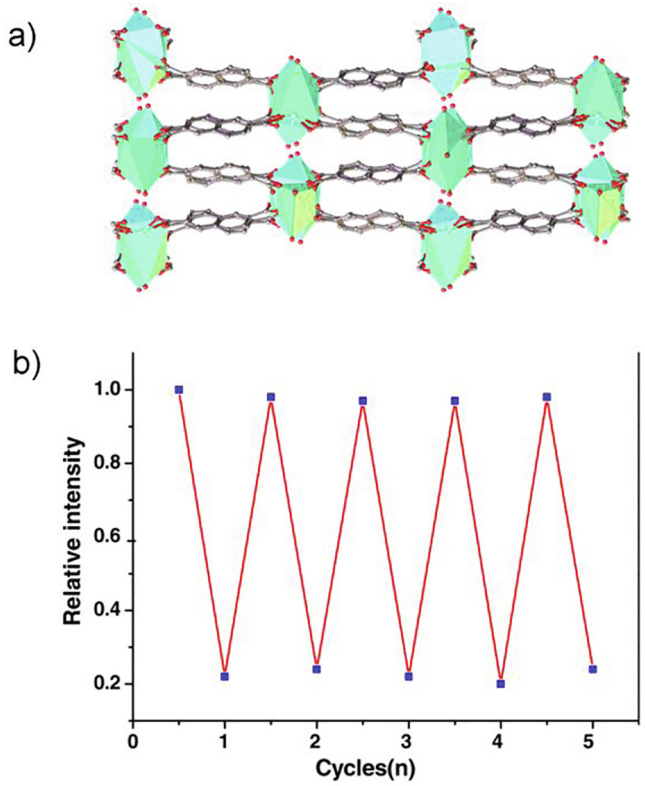


**Fig. 6. a)** Structure of Eu-NDC as viewed along the crystallographic *a*-axis.[106] **b)** Recyclability over 5 cycles of the Eu-NDC thin film immersed in 100 μM picric acid. Reproduced with permission from Ref. [105]. Copyright 2017, Springer Nature.

mechanism involves photoinduced electron transfer (PET) from the excited state organic linker to the DNT and DMNB molecules.

Following this first report of MOFs being used for detection of explosives, MOFs have been reported to be applicable as efficient sensors for many explosive compounds, including picric acid, which also represents a well-known environmental pollutant used in the dye industry.[101] The use of luminescent MOF films for this purpose has been an area of much research. MOF thin films offer some advantages over MOFs which have been synthesised in bulk by solvothermal methods. Electrodeposition allows MOF films to be prepared under mild conditions, at room temperature, with short reaction times of as little as a few seconds.[102] Moreover, electrodeposition of MOFs can be used to selectively form MOFs in instances when more than one phase can be formed from the reagents, as reported by Dincă and co-workers for electrodeposition of MOF-5 [103,194]. This method can be used to yield uniform, well-adhered films of MOFs. In terms of their use as sensors, MOF thin films can easily be separated from the analyte solution by removal of the film, and in many cases the material can then be washed and reused.[104]

An example of the use of an electrodeposited luminescent MOF was reported by Yang and co-workers, using the MOF $[Eu_4(NDC)_6(H_2O)_5]\cdot 3H_2O$ (Eu-NDC; $NDC^{2-}$ = naphthalene-2,6-dicarboxylate). [105] Eu-NDC was first reported by Jin and co-workers in 2006. [106] The structure of Eu-NDC comprises channels with a compressed honeycomb-like shape, which run parallel to the crystallographic *a*-axis (Fig. 6a)).

Yang and co-workers reported the synthesis of Eu-NDC by electrochemical methods on to the surface of fluorine-doped tin oxide (FTO) in 20 s.[105] Eu-NDC showed metal-centred luminescence under UV light irradiation ($\lambda_{ex}$ = 355 nm). In response to the presence of picric acid dissolved in water samples, the MOF displayed luminescence quenching, with a detection limit of 0.67 μM. Furthermore, the MOF thin film could be washed and reused 5 times with no significant decrease in luminescence quenching (Fig. 6b)).

### 3.1.2. Sensing of metal ions

Many metal ions are toxic to human, plant and animal life, and as a result, the development of stable, reusable materials, which can rapidly detect the presence of metal ions at low concentration is desirable. Metal ions such as $Li^{I}$, $Cr^{VI}$, $Hg^{II}$, $Cd^{II}$ and $Pb^{II}$ are dangerous to the environment, livestock and human health. Other ions are biologically essential, such as $Cu^{II}$, $Zn^{II}$, or $Fe^{II}$, but are harmful at higher concentrations. Luminescent MOFs have been reported to function as effective sensors for a wide range of metal ions. In some cases, selective sensing of specific metal ions over other analytes is possible.[107] Selective sensing of ions has also been accomplished, in fact, MOFs have been reported to be capable of discriminating between $Fe^{II}$ and $Fe^{III}$ ions.[108]

As previously mentioned, a common mechanism for luminescence sensing of metal ions by MOFs is through interactions between the analyte metal ions and the organic linker of the MOF structure. This interaction can lead to quenching or enhancement of the MOF luminescence, or a shift in the wavelength at which the MOF emits light. In some rarer cases, the luminescence response can even be observed by the naked eye.[109,110] One approach which can increase the ability of MOFs to sense metal cations involves the functionalisation of organic linkers, for example, through introduction of functional groups containing Lewis-basic N, O or S atoms.

Nitrogen- and sulfur-containing linkers have been reported as promising linkers for selective detection of $Hg^{II}$ ions, which is desirable due to the toxicity of these ions, and their potential for bioaccumulation. One example was reported by Wang and co-workers.[111] Reaction of $Cd(NO_3)_2\cdot 6H_2O$ and the organic ligand, 4,4′,4″-s-triazine-1,3,5-triyltri-p-aminobenzoate ($TATAB^{3-}$) gave a porous, luminescent MOF (Cd-TATAB) (Fig. 7). The organic linker features two kinds of Lewis-basic functional moieties, involving the central triazine ring and the surrounding amino functionalities (Fig. 7). Due to the high affinity of $Hg^{II}$ ions for nitrogen donors, and the spatial orientation of the nitrogen atoms in $TATAB^{3-}$, this MOF facilitates selective detection of $Hg^{II}$ ions (Fig. 7c)), even in the presence of several other transition metal ions. In this case, the characteristic luminescence response arises from LMCT effects, which are influenced by $Hg^{II}\cdot\cdot N$ interactions between the metal ions and the framework structure, leading to luminescence quenching and a red shift of the MOF-derived luminescence (Fig. 7d)).

In 2013, Su and co-workers reported a Zn-containing MOF, IFMC-28 (IFMC = Institute of Functional Materials Chemistry), using 3,4-dimethylthieno[2,3-*b*]thiophene-2,5-dicarboxylate ($DMTDC^{2-}$) as a linker (Fig. 8).[112] The Lewis-basic sulfur sites of the thienothiophene linker were identified as potential coordination sites for the selective chelation of metal ions. IFMC-28 showed selective adsorption of $Cu^{II}$ ions over other metal ions, such as $Pb^{II}$, $Ni^{II}$, $Co^{II}$, $Mn^{II}$, $Mg^{II}$ and $Cd^{II}$ ions (Fig. 8b)). This selective adsorption behaviour was not observed in experiments using the isoreticular MOFs, MOF-5 or IRMOF-3, as controls (Fig. 8c)) and was therefore attributed to favourable binding energies between sulfur atoms and metal ions. This selective absorption behaviour could be applied to the use of IFMC-28 as an ion chromatographic column, which selectively favoured adsorption of $Cu^{II}$ ions over $Co^{II}$ ions, giving an efficient method of separating $Co^{II}$ ions from $Cu^{II}$ ions (inset, Fig. 8c)).

Many MOFs based on $d^{10}$ metal ions have been reported to display luminescence sensing as a result of interactions between functionalised ligands and analyte metal ions. For example, Zhang and co-workers reported two Cd- and Zn-based MOFs which can

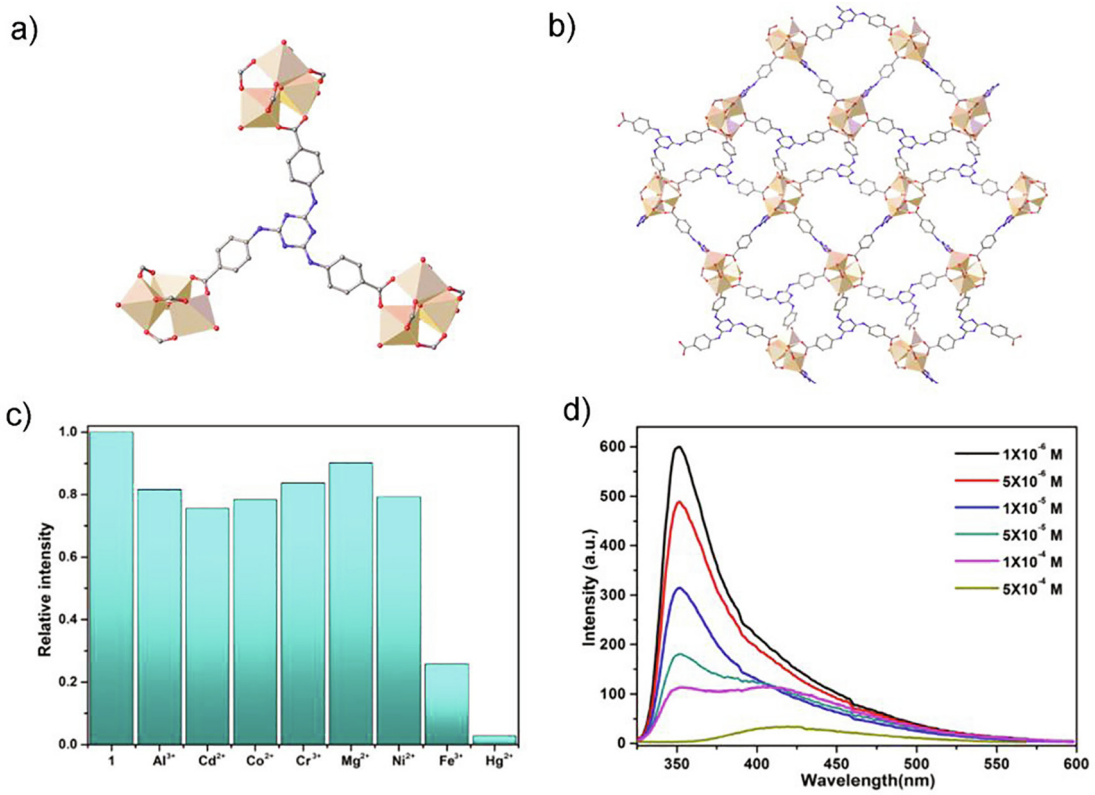


**Fig. 7. a)** Ligand and inorganic SBU of $Cd^{II}$-based MOF, Cd-TATAB **b)** Structure of the MOF **c)** relative fluorescence intensity of Cd-TATAB (1) MOF in response to the presence of metal ions **d)** Changes in fluorescence spectra of $Cd^{II}$-MOF in response to increasing $Hg^{II}$ concentration. Reproduced with permission from Ref. [111]. Copyright 2018, Elsevier B.V..

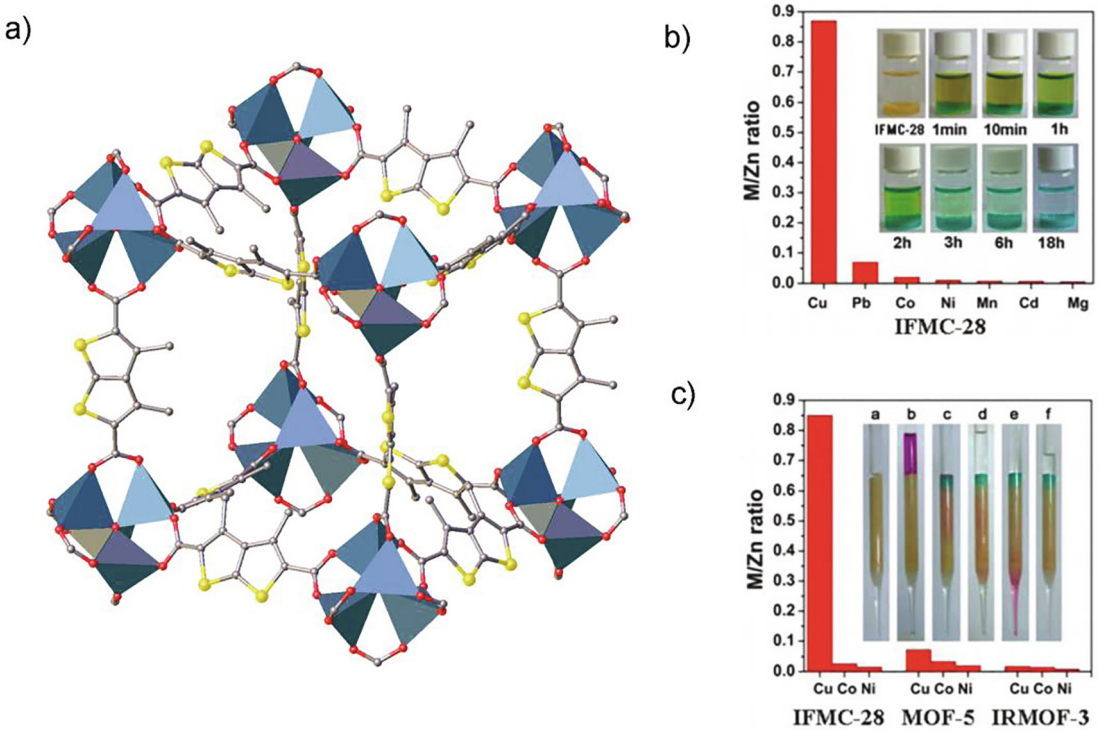


**Fig. 8. a)** Structure of IFMC-28 **b)** Metal ion absorption selectivity (graph) and $Cu^{II}$ sorption over time when IFMC-28 was immersed in $CuCl_2$ solution (inset) **c)** Comparison of absorption of metal ions by IFMC-28, MOF-5 and IRMOF-3 and separation of $Cu^{II}$ and $Co^{II}$ ions by the MOF-based chromatography column (inset). Reproduced with permission from Ref. [112]. Copyright, Royal Society of Chemistry, 2013.

efficiently sense a range of transition metal ions.[113] These MOFs incorporate the ligand benzo-(1,2;4,5)-bis(thiophene-2′-carboxy late) ($BBTC^{2-}$), and two different ancillary ligands. Both MOFs display luminescence quenching effects in response to $Hg^{II}$, $Cu^{II}$ and $Cr^{VI}$ ions. These ions can be detected selectively by the MOFs from aqueous solutions containing other analytes. Luminescence quenching was also observed in response to the presence of the organic molecule salicylaldehyde in ethanol solution. Furthermore, in the case of $Cr^{VI}$, $Hg^{II}$ and salicylaldehyde, the sensing behaviour could be reproduced after washing the MOFs, demonstrating facile recyclability of the system.

The detection of toxic anions in wastewater is important to prevent environmental contamination, and MOFs have been reported that can detect harmful pollutants such as $Cr_2O_7^{2-}$ and $CrO_4^{2-}$.[88,114] These ions present a serious risk to human health, causing DNA damage and cancer.[115] Li and co-workers have reported the synthesis of a luminescent Zr-based MOF, BUT-39 (BUT = Beijing University of Technology) which contains a tritopic imidazole ligand.[116] The luminescence in the MOF arises from ligand-centred emission. BUT-39 could selectively detect $Hg^{II}$ and $Fe^{III}$ ions through luminescence quenching effects. In terms of anion sensing, BUT-39 showed a selective sensing ability towards $Cr_2O_7^{2-}$, as the MOF luminescence was quenched by 99% in response to this anion. In addition to this luminescence sensing response, the MOF also facilitated rapid removal of $Cr_2O_7^{2-}$ from water. This dual potential of sensing and absorbing harmful ions from aqueous solutions demonstrates some of the advantages of utilising porous, luminescent MOFs as sensor materials.

### 3.2. MOFs for tunable light emitting devices

The emission of MOFs can be tuned using several different methods, including by linker variation, incorporation of dopant metal ions into the SBU of MOFs,[117,118] and absorption of guests which alter the luminescence properties of the MOFs.[119]

A strategy that has been effective in designing MOFs that are characterised by tunable light emission involves the synthesis of Ln-MOFs using multiple different lanthanide ions, to give mixed-lanthanide MOFs.[120,121] Every $Ln^{III}$ ion, except $La^{III}$ and $Lu^{III}$, is photoluminescent. This luminescence can be observed in the UV region ($Gd^{III}$), in the visible region ($Pr^{III}$, $Sm^{III}$, $Eu^{III}$, $Tb^{III}$, $Dy^{III}$, $Ho^{III}$, $Tm^{III}$) or in the near-infrared (NIR) region ($Pr^{III}$, $Nd^{III}$, $Ho^{III}$, $Er^{III}$, $Yb^{III}$).[67] These ions can be categorised as triplet state emitters whereby the emission is often referred to as ‘metal-centred’ or as ‘lanthanide delayed luminescence’; as crystal field effects are minimal and the emission generally arises from the deactivation of the lanthanide’s excited state. Due to their visible, ‘bright’ luminescence (which is due to their long-lifetimes in the millisecond time range, which overcomes autofluorescence from other shorter lived emitters and from light scattering), $Eu^{III}$ (red emission) and $Tb^{III}$ (green emission) ions in particular have been studied with great interest. Further, the use of most conventional and commercially available spectrometers allows for their emission to be recorded without the need of special detectors (as is the case for some of the NIR emitting ions). However, a drawback to the use of the lanthanides is that their excited states can easily be quenched by O–H oscillators of coordinating solvent molecules, particularly water and alcohols, as their narrow energy gaps can be quenched. The often observed on and off emission characteristics associated with binding or displacement of solvent molecules is often exploited in functional materials including MOFs.[122]

In some cases it is possible to dope different lanthanide ions into a MOF without changing the framework structure.[123] Facile synthesis of mixed-lanthanide MOFs with varying ratios of lanthanide ions can be achieved by controlling the stoichiometry of the reactant lanthanide ions during synthesis.[124–126] In mixed-lanthanide MOFs, multiple luminescence emission bands are observed from the different lanthanide ions in the structure, allowing modulation of overall emission colour.[127–130] Thus, strategic combination of lanthanide ions that emit light in different regions of the visible spectrum allows the luminescence output of the MOFs to be specifically tuned, depending on the desired application; particularly significant work has been dedicated to the use of lanthanide-based MOFs or related soft materials as white light emitters.[131–133]

A vast majority of known luminescent materials only show emission in one part of the visible region of the electromagnetic spectrum. Su and co-workers reported a series of isostructural mixed-lanthanide MOFs, which can be tuned towards a range of emission colours.[134] The MOFs in this series have the general formula $[Ln_nLn'_{1-n}(TTP)_2{\cdot}H_2O]Cl_3$•solvent (TTP = 1′,1″-(2,4,6-trimethylbenzene-1,3,5-triyl)tris(methylene)tris(pyridine-4(1H)-one)). Mixed-metal MOFs were synthesised using three combinations of two different ions; $Eu^{III}$ and $Tb^{III}$, $Eu^{III}$ and $Gd^{III}$, $Gd^{III}$ and $Tb^{III}$ ions. The structure of the MOF consists of seven-coordinate $Ln^{III}$ ions, with pentagonal-bipyramidal geometry. Each $Ln^{III}$ is coordinated by six oxygen atoms from six different TTP ligands and one water molecule. The MOF forms one-dimensional chains with channels within (Fig. 9a)).

The TTP ligand behaves as an antenna for photosensitisation of the $Eu^{III}$ (red emission) and $Tb^{III}$ (green emission) ions in the MOF (Fig. 9b)). The presence of methylene groups linking the pyridone groups to the core benzene rings allows each pyridone group to function as an independent sensitising antenna. Coordination of a pyridine group to $Gd^{III}$, which is non-emissive in the visible region, results in ligand-centred blue emission from the pyridone group. Changing the ratios of the lanthanide ions in the structure allowed the colour of the MOF luminescence to be varied across the RGB triangle.

Materials that exhibit white light emission are desirable due to their applications in displays and solid-state lighting.[135,136] Often, sources of white light are achieved by combining light sources, however this has drawbacks due to high costs and variations in colour.[137] Therefore the design of materials which can emit white light is a current topic of much research in the field of luminescent materials.[138]

In multicomponent MOFs, which contain more than one type of linker molecule, the emission of the MOF can be tuned by variation of each of the linkers in the structure independently, affording great control over the luminescence output of the material. For example, Telfer and co-workers have reported a multicomponent MOF composed of three structurally different linkers, and demonstrated that the luminescence properties of this MOF can be controlled both by linker modification and guest binding (Fig. 10).[139] The constitutional composition of this MOF, abbreviated as MUF-77 (MUF; Massey University Framework) is given by the formula $[Zn_4O(hxtt)_{4/3}(BPDC)_{1/2}(BDC)_{1/2}]$ (hxtt = 5,5,10,10,15,15-hexaalkyl-10,15-dihydro-5*H*-diindeno[1,2-a:1′,2′-c]fluorene-2,7,12-tricarboxylic acid (alkyl = methyl, butyl, hexyl or octyl)), $BPDC^{2-}$ = 4,4′-biphenyldicarboxylate). Prior to modification of the linkers, the MOF showed blue emission. Introduction of a guanidine functional group to the $BPDC^{2-}$ linker moiety resulted in yellow emission from the MOF, while addition of a $–NH_2$ functional group to the $BDC^{2-}$ linker gave blue fluorescence. Combining the guanidine functionalised $BPDC^{2-}$ and the amine functionalised $BDC^{2-}$ group gave a white light emitting MOF. Additionally, the luminescence of MUF-77 could be tuned by interactions with guest molecules in the framework. In response to the presence of nitrobenzene, which interacts with the MOF through hydrogen bonding, the emission of the MOF was quenched. Interestingly, this quenching effect was stronger for the yellow emission band of the MOF, causing the luminescence output of the MOF to shift to a blue colour.

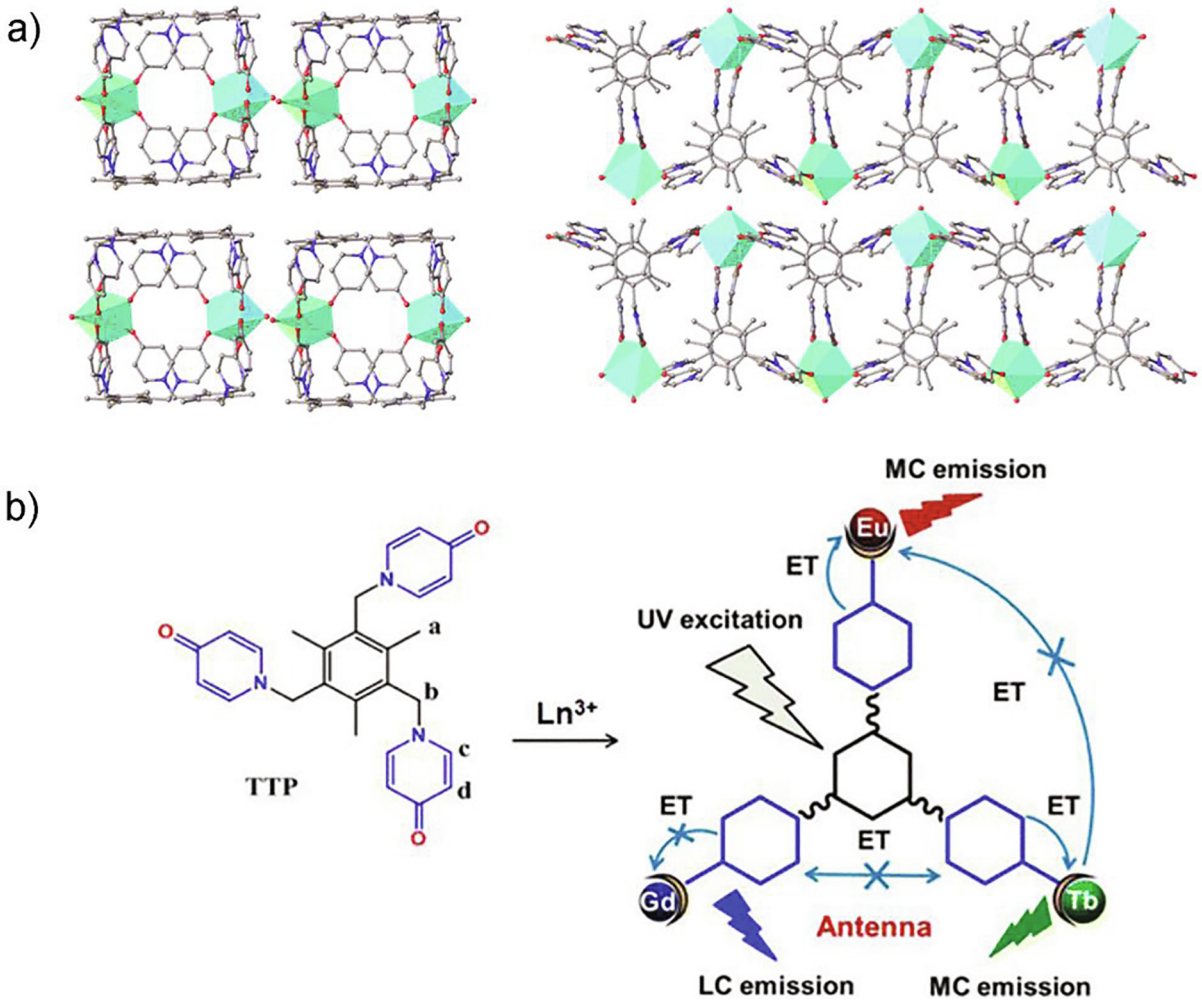


**Fig. 9. a)** Crystal structure of isostructural MOFs with the general formula $[Ln_nLn'_{1n}(TTP)_2{\cdot}H_2O]Cl_3{\cdot}$solvent, showing their packing mode. **b)** Synthesis of the MOFs from TTP, showing energy transfer processes. Reproduced with permission from Ref. [134]. Copyright 2015, American Chemical Society.

As demonstrated by some previously mentioned examples, the inclusion of guest molecules in MOFs also provides a method of tuning their photochemistry. The porosity of MOFs allows for incorporation of guest molecules which can influence the luminescence output of the material. For example, Qian and co-workers have reported that encapsulation of dye molecules into the structure of MOFs gives a method of modulating the colour of the luminescence output of the material.[140] Two cationic dyes, acriflavine (AF), which emits green light, and 4-(*p*-dimethylamines tyryl-1-methylpyridinium (DSM), which emits red light, were encapsulated in the anionic framework ZJU-28 (ZJU = Zhejiang University). ZJU-28 is an anionic MOF, with the formula $(Me_2NH_2)_3[In_3(BTB)_4]{\cdot}12DMF{\cdot}22H_2O$ ($BTB^{3-}$ = 4,4′,4′′-benzene-1,3,5-tri yl-tribenzoate).[141] Prior to encapsulation of dyes, ZJU-28 emits blue light upon excitation with UV light (λ = 365 nm). Incorporation of the DSM dye into the structure of ZJU-28 gives tunable light emission, with blue emission observed at low dye concentration, and purple emission at high dye concentration.[140] A similar effect is observed when AF is encapsulated into the MOF, with green emission observed at high AF concentration. Encapsulation of the two dyes, AF and DSM, into ZJU-28, gives a mixed-dye exchanged MOF which emits white light. The potential of this material in white light emitting devices was also demonstrated by coating a UV-LED (LED = light emitting diode) with the mixed-dye-encapsulated MOF, resulting in warm white light emission from the MOF-coated LED.

Recently, MOFs have been reported for their application as organic light emitting diodes (OLEDs). OLEDs and LEDs are devices which generate light in response to an electric current. LEDs are typically constructed from semiconductor materials such as GaN or AlGaN, with the colour of light emitted depending on the band gap of the material. The emissive components of OLEDs are films of organic compounds or polymers. Compared to LEDs, which are typically rigid systems, OLEDs can possess increased flexibility, which, in principle, allows for displays that can be bent and rolled up.[142] Furthermore, OLEDs can be designed to be transparent materials.[143]

In 2018, Douhal and co-workers reported OLEDs based on a Zr-based MOF, Zr-NDC.[144] The structure of Zr-NDC is composed of $[Zr_6(\mu_3\text{-}O)_4(\mu_3\text{-}OH)_4(\mu\text{-}COO)_{12}]$ SBUs, which are 12-fold connected by the $NDC^{2-}$ organic linkers. This MOF displays electroluminescence, a property which is relatively rare in MOFs. Incorporation of dye molecules as guests into the MOF pores can effectively tune the optoelectronic properties of this material. Two different dye molecules were encapsulated into the MOF pores, Coumarin 153 (C153) and 4-(dicyanomethylene-2-methyl-6-(4-dimethylaminos tyryl)-4H-pyran (DCM). In the MOFs with encapsulated dyes, C153@Zr-NDC and DCM@Zr-NDC, two different emission bands are observed in the photoluminescence spectra, blue luminescence originating from the Zr-NDC MOF, and red luminescence from the encapsulated dye molecules. The photoluminescence bands of both dyes are shifted in the MOF environment compared to the pure

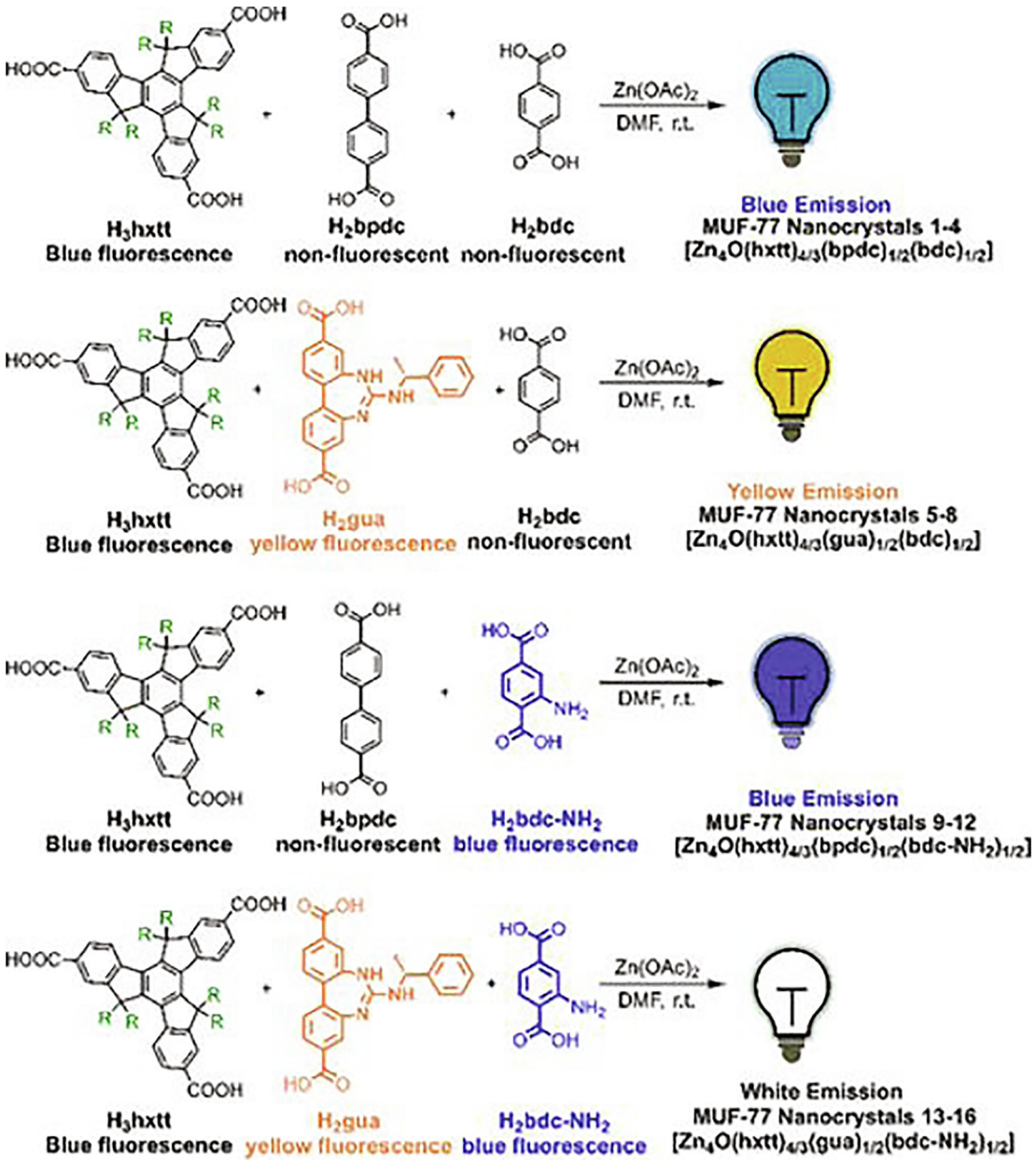


**Fig. 10.** Synthesis of luminescent MUF-77 nanocrystals and their luminescence output colours (R = methyl, butyl, hexyl or octyl groups). Reproduced with permission from Ref. [139]. Copyright 2018, American Chemical Society.

dyes in the solid state, indicating that interaction occurs between the MOF and the dyes in their pores.

To investigate the electroluminescence of Zr-NDC and the dye-encapsulated analogues, Douhal and co-workers designed light emitting devices with the MOF as a light emitting layer in a polymer matrix. The MOF displayed electroluminescence that could be modified by dye encapsulation. The dye encapsulated MOFs did not show a change in colour of electroluminescence, however, the electroluminescence intensity was increased in C153@Zr-NDC and DCM@Zr-NDC.

## 4. MOFs as photocatalysts

In view of sociologically important sustainable energy-related applications, MOF-based research activities can be directed towards artificial photosynthetic systems. Artificial photosynthetic systems that convert light into chemical energy, producing molecular $O_2$ and $H_2$, provide arguably the most attractive approach to green and renewable energy technologies. Photosynthesis is the process by which plants, algae and some bacteria use light energy to split water, and use the electrons and protons produced for the reduction of $CO_2$ to produce sugars. The process stores energy in chemical bonds. Insights into molecular details of these conversions can guide us towards employing solar energy to produce fuels, whereby the term 'fuel' in a broader sense can be thought of as a reduced molecule that can be oxidised, to produce desired compounds or energy as required. The replication in any artificial photosynthetic analogue is scientifically highly challenging but can be rendered more manageable when the overall process is separated into distinct sequential, partial processes: a) light harvesting, b) charge separation, c) reaction involving the positive cation

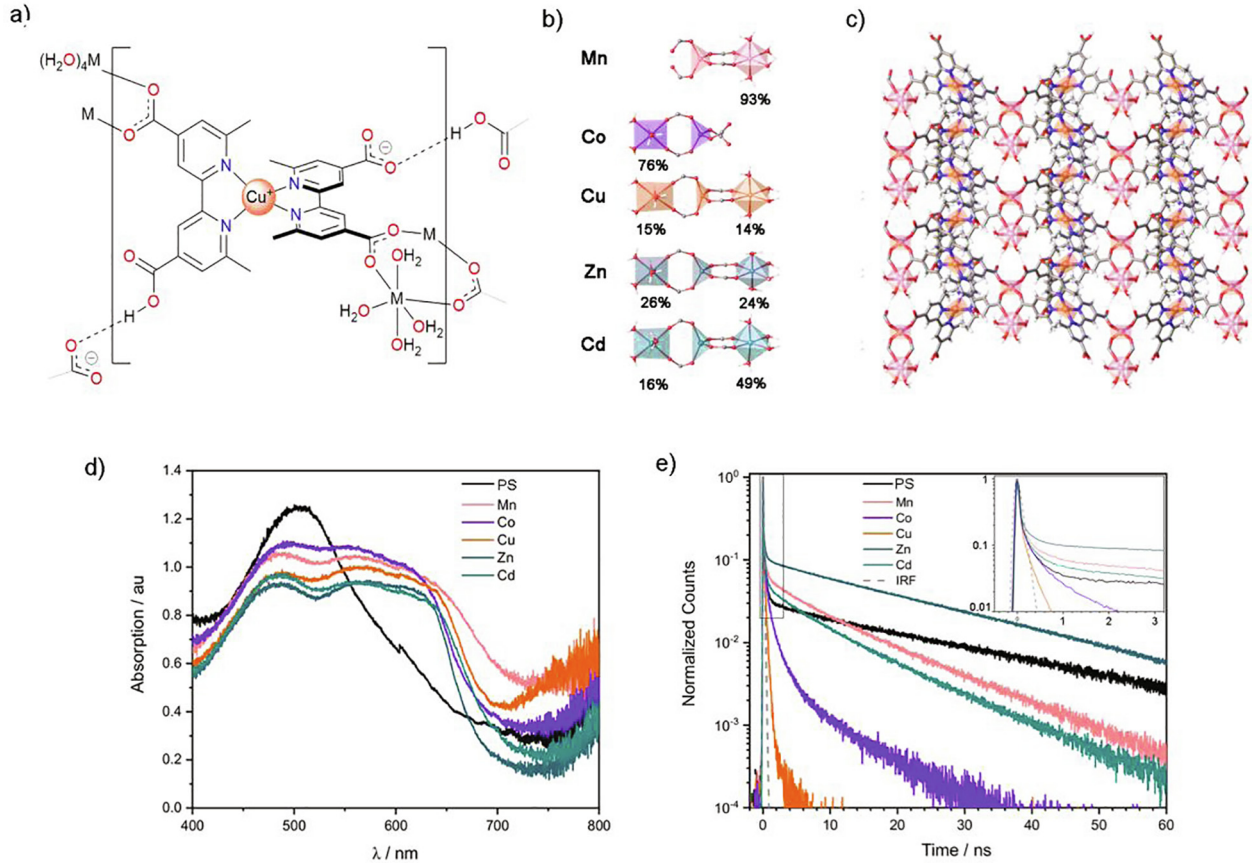


**Fig. 11. a)-c)** Structural representations of $[Cu(H_{1-x}2,2'\text{-DMBP})_2M_{0.5}][M(OH_2)_4]_x$ (M = $Mn^{II}$, $Co^{II}$, $Cu^{II}$, $Zn^{II}$, or $Cd^{II}$) **a)** Structural role of the $Cu^{I}$-photosensitiser. **b)** Coordination environments of metal ions in the SBUs and the occupancies of the $[M^{II}(OH_2)]$ moieties. Only one of the chemically equivalent (though crystallographically distinct) $[M(OH_2)_4]$ moieties can be occupied per SBU. **c)** Layers of the $Mn^{II}$-based MOF featuring $[Cu^{I}(H_2}2,2'\text{-DMBP})_2]PF_6$ metallolinkers **c)** Absorption spectra and **d)** normalised photoluminescence decay of $[Cu^{I}(H_2}2,2'\text{-DMBP})_2]PF_6$ (PS) and MOFs (inset: initial decay characteristics) (IRF = instrument response function). Adapted with permission from Ref. [145]. Copyright 2020, American Chemical Society.

'hole' at the catalytic centre to oxidise a suitable electron donor molecule (water or other donor molecules) and d) reactions involving the mobilised electrons to produce a desired compound via the reductive process. Thus, by conceptualizing 'artificial photosynthesis' into these modular processes, catalytic oxidative and reductive processes may be developed and combined to give a highly efficient, optimised overall redox system.

The influence of the inorganic SBUs on the optoelectronic properties of MOFs was recently exemplified using five isostructural 2D MOFs which incorporate a $Cu^{I}$ metallo-linker, $[Cu^{I}(H_2}2,2'\text{-DMBP})_2]PF_6$ ($H_2$4,'-DMBP = 6,6′-dimethyl-2,2′-bipyridine-4,4′-dicarboxylic acid) (Fig. 11).[145] The MOFs, $[Cu(H_{1-x}4,4'\text{-DMBP})_2M_{0.5}][M(OH_2)_4]_x$ (M = $Mn^{II}$ (x = 0.47), $Co^{II}$ (x = 0.38), $Cu^{II}$ (x = 0.14), $Zn^{II}$ (x = 0.25), or $Cd^{II}$ (x = 0.32)), feature mixed mono- and dinuclear SBUs (Fig. 11a)). The compounds exhibit broad absorption in the visible region (Fig. 11c)) and emission centred at 728 nm. Compared to the parent photosensitiser, the MOFs' rigidity enhances intersystem crossing from the singlet to the triplet state and enables higher radiative decay rates, which depend on the nuclearity of the SBU and O–H oscillations of coordinated water molecules. Quantum yields depend on the chemical nature of the SBU, and are up to six times higher for the $Zn^{II}$-MOF than for $[Cu^{I}(H_2}4,4'\text{-DMBP})_2]PF_6$. The shortest triplet excited state lifetimes are observed for the $Cu^{II}$- and $Co^{II}$- systems, as the excited states are quenched by rapid electron transfers to the SBU (Fig. 11d)). This series of MOFs demonstrates the potential for tuning photochemical properties by variation of the nature of the metal ions within the inorganic SBUs.

### 4.1. $CO_2$ reduction

Due to rising levels of atmospheric $CO_2$ from fossil fuel combustion, and the need to curb the associated rise in global temperatures, research into technologies that can capture $CO_2$ and convert it to value-added products is a source of high scientific and societal interest. Fixation of $CO_2$ to form valuable products such as CO and methanol has the potential to replace or alter current methods of synthesising these products, which use conventional fossil fuels as a feedstock.[146,147] However, the thermodynamic energy barriers associated with the conversion of $CO_2$ currently present a major challenge in implementing these new sustainable and cost-effective technologies.

MOFs have been explored as materials that can catalyse the reduction of $CO_2$ using visible light as an energy source.[148,149] Early catalysts for $CO_2$ reduction involved various metals or metal oxides such as $TiO_2$,[150] followed by the development of molecular homogenous catalysts.[151] However, the use of heterogenous photocatalysts for $CO_2$ reduction offers several advantages over homogenous catalysts.

The advantages of MOFs as heterogenous catalysts arise from their intrinsic properties and their ordered and well-defined nature, whereby associated reticular synthesis concepts offer some degree of synthetic control during assembly of the materials. This approach may allow the preparation of materials in which the components for photocatalysis, for example the photosensitiser, catalyst and sacrificial electron donor, can be oriented in an ordered and well-defined manner, thus optimising electron trans-

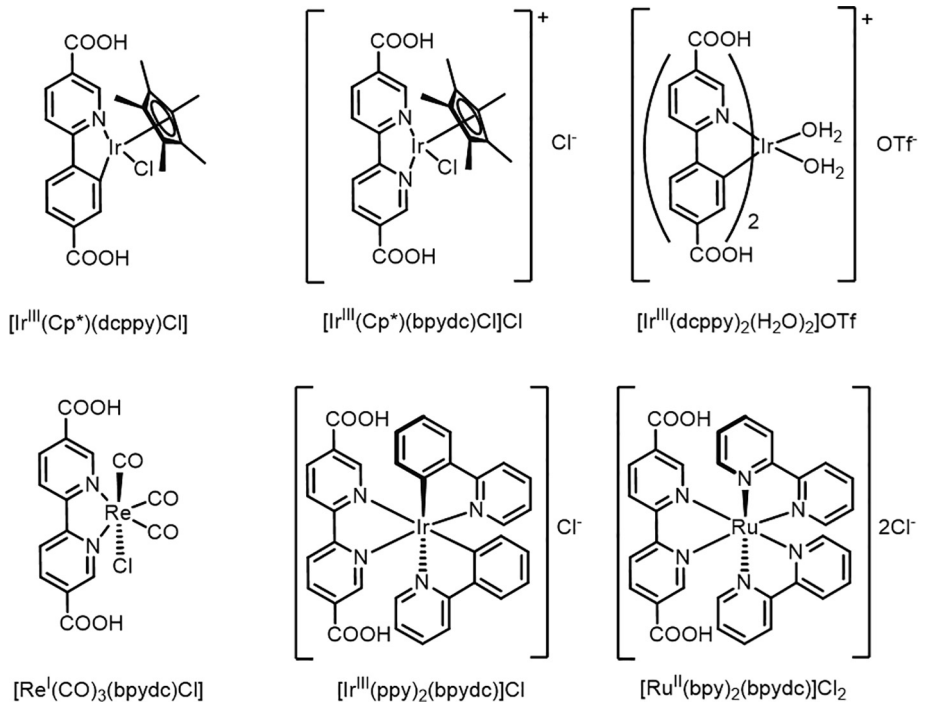


**Fig. 12.** $Ir^{III}$, $Re^{I}$ and $Ru^{II}$ metalloligands used by Lin and co-workers in the synthesis of doped UiO-67 frameworks.[153]

fer to the active site. The dimensions of the components determine the porosity and diffusion characteristics in the materials. Catalytic transformations may occur in confined spaces of molecular-sized cavities, involving structural intermediates and moieties that may relate to those of molecular catalysts, or which may not be attainable in condensed liquid phases. Hence, MOFs may provide synthetic avenues to bio-inspired materials that replicate some of the key features of enzymatic catalysts.

The development of photocatalytic MOFs for $CO_2$ reduction represents an area of intense research, and as a result, different generations of photoactive MOFs have emerged.[152] First generation MOFs for photocatalytic $CO_2$ reduction employ the strategy of immobilising molecular photocatalysts in MOFs. First generation MOFs overcome some issues that arise when using homogenous catalysts, preventing dimerization of catalysts and the resulting loss of catalytic activity. Additionally, the environment within

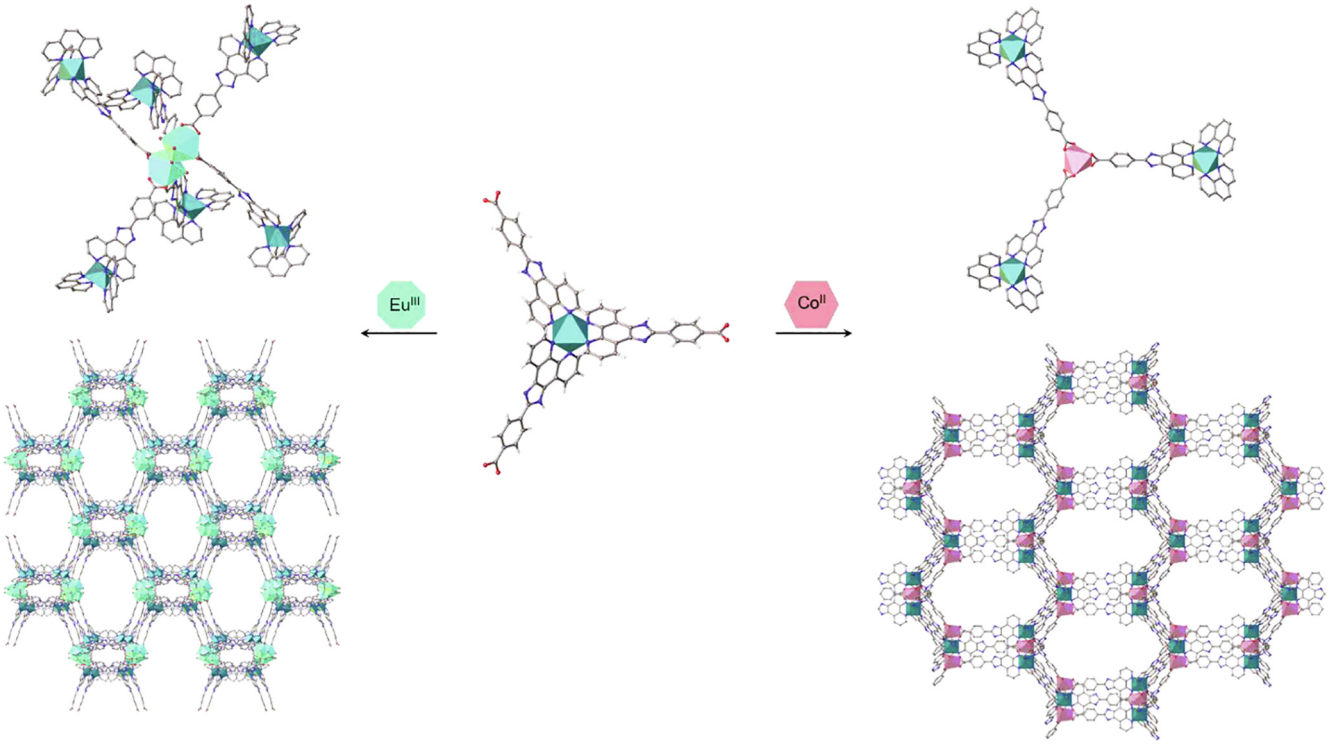


**Fig. 13.** Structures of MOFs formed upon reaction of a $\{Ru^{II}(phen)_3\}$-derived ligand with $Eu^{III}$ salts (left)[53] and $Co^{II}$ salts (right).[52]

MOFs offers advantages for photocatalytic reactions, such as high densities of catalytic active sites and good light penetration into their crystalline structures.[152]

Second generation photoactive MOFs are those which are capable of absorbing light in the visible region of the spectrum.[152] This characteristic is important in order to carry out photocatalysis efficiently using solar light as an energy source. Absorption of light by MOFs is typically tuned by variation of the organic linker in the system, emphasising the advantages of the tunable optical properties of MOFs. Third generation photocatalytic MOFs focus on electronic efficiency, by aiming to optimise the transfer of energy from the photosensitiser to the catalytic active site.[152] These materials should have charge separated states with lifetimes that are long enough to facilitate transfer of electrons to the $CO_2$ substrate.

In 2011, Lin and co-workers reported the first example of MOFs that could perform as heterogenous catalysts for $H_2O$ oxidation, photocatalytic $CO_2$ reduction and light-driven organic reactions.[153] A series of stable, porous heterogenous catalysts were prepared by incorporating various catalytically active complexes as metalloligands into the UiO-67[154] (UiO = Universitetet i Oslo) framework, $[Zr_6O_4(OH)_4(BPDC)_6]$ (Fig. 12). Varying the molecular dyes used as metalloligands changed the catalytic behaviour of the MOF. For example, using $[Re^{I}(CO)_3(bpydc)Cl]$ (bpydc = 2,2′-bi pyriine-5,5′-dicarboxylic acid) as a metalloligand enabled the MOF to perform as a heterogeneous photocatalyst for reduction of $CO_2$. A turnover number (TON) of 10.9 was recorded for the Re-doped MOF over a 20 h reaction period, which is over three times higher than that recorded for $[Re^{I}(CO)_3(bpydc)Cl]$ in solution over the same time period. Incorporating linkers which were previously established as molecular water oxidation catalysts (WOCs), such as $[Ir^{III}(Cp^*)(dcppy)Cl]$ ($Cp^{*-}$ = pentamethylcyclopentadienyl, dcppy = 2-phenylpyridine-5,4′-dicarboxylic acid), $[Ir^{III}(Cp^*)(bpydc)Cl]^+$ and $[Ir^{III}(dcppy)_2(H_2O)_2]^+$, led to MOFs which were capable of performing as $H_2O$ oxidation catalysts. The highest turnover frequency was observed for the MOF which incorporates $[Ir^{III}(Cp^*)(dcppy)Cl]$, with a turnover frequency (TOF) of 4.8 $h^{-1}$ recorded over the first 3 h. In addition, the MOFs synthesised with $[Ir^{III}(ppy)_2(bpydc)]^+$ (ppy = 2-phenylpyridine) and $[Ru^{II}(bpy)_2(bpydc)]^{2+}$ (bpy = 2,2′-bipyridine) were capable of catalysing photochemical aza-Henry reactions, aerobic amine coupling and sulfide photooxidations.[153]

In 2018, Zheng and co-workers reported the synthesis of a novel Eu-based MOF with a $\{Ru(phen)_3\}$-derived (phen = phena throline) ligand, [Ru(4-(1H-imidazo[4,5-*f*][1,10]phenanthrolin-2-yl)benzoate)$_3$] and dinuclear $\{Eu_2^{III}\}$ SBUs (Fig. 13)).[53] Europium was chosen due to the favourable reduction potential of $Eu^{II}$ for catalytic reduction reactions,[155,156] while the rational for use of the $Ru(phen)_3$-derived ligand was the redox activity and excited state lifetime of ruthenium polypyridine complexes.[157] Zheng and co-workers report the synthesis of a $Ru^{II}/Eu^{III}$ MOF, in which the carboxylate-bearing $Ru^{II}$-metalloligands bridge dinuclear $\{Eu_2^{III}\}$ moieties, to give a MOF with large channels that penetrate the material (Fig. 13)).[53] Each $Eu^{III}$ ion in the structure is nine-coordinate, and one $\mu_2$-$H_2O$ bridges the two ions in each dinuclear $\{Eu_2^{III}\}$ unit. This MOF efficiently catalyses the reduction $CO_2$ to formate upon photoirradiation with visible light ($\lambda_{ex}$ = 420–800 nm). Upon irradiation, the $Ru^{II}$ metalloligand is excited to its $^3$MLCT excited state, followed by PET from the ligand excited state to the $[Eu^{III}$-$H_2O$-$Eu^{III}]$ unit. Transfer of two electrons results in the reduction of this unit to a photogenerated dinuclear $[Eu^{II}$-$H_2O$-$Eu^{II}]$ species, which reduces $CO_2$ to formate. The catalytic cycle is completed by reduction of the $Ru^{III}$ ion back to $Ru^{II}$ by a sacrificial electron donor. The same metalloligand was also employed for the formation of a $Co^{II}$-based MOF that is characterised by hexagonal accessible helical one-dimensional channels (Fig. 13). Its structural characteristics facilitate relatively high $CO_2$ uptake capacities and selectivity over $N_2$. The photoactive porous material retains the photophysical properties of the $Ru^{II}$ nodes giving rise to emission centred at 620 nm and photoactivity associated with the $^3$MLCT states.[52] It is further noteworthy that the bifunctional phenanthroline-carboxylate ligand itself can be applied for the synthesis of photoluminescent Zn- and Mn-based MOFs displaying high $CO_2$ adsorption capacities associated with structural framework flexibility.[158]

Though $Ru^{II}$-based linkers have shown great potential as photosensitising ligands in photoactive MOFs, the development of catalysts using earth abundant metals is desirable. Fe-containing MOFs

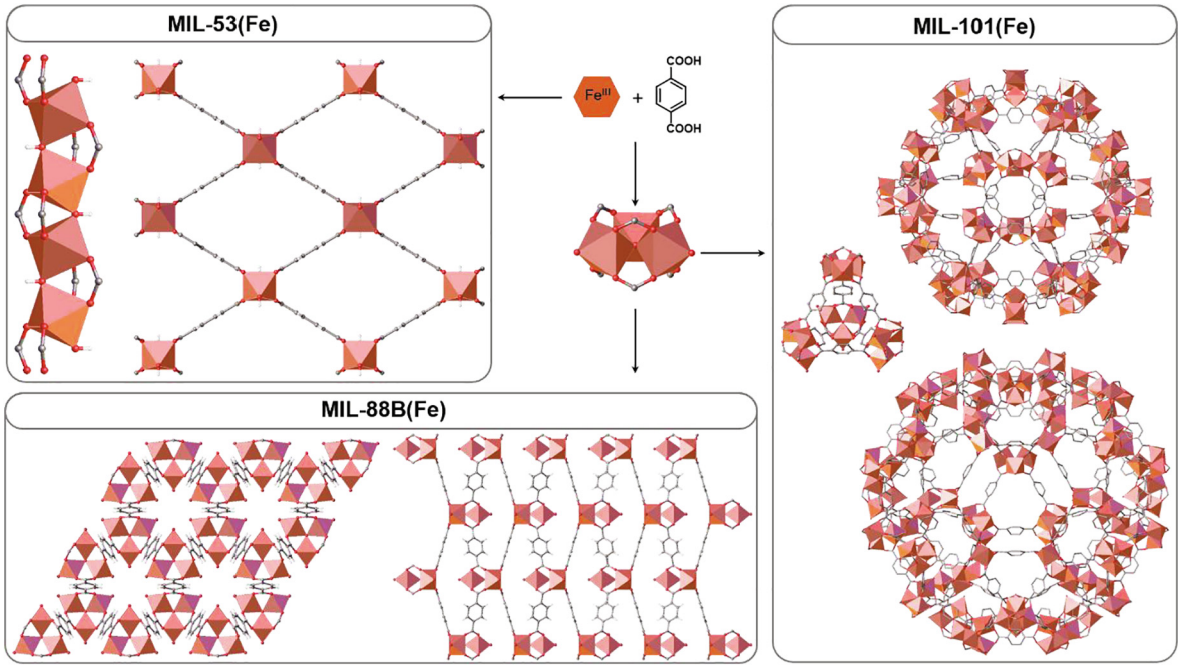


**Fig. 14.** Structural differences between MIL-53(Fe),[160] MIL-88B(Fe)[161] and MIL-101(Fe).[162]

fulfil the criteria of containing earth abundant metals and have the added advantage that it is possible to use visible light to excite the Fe oxo-clusters of these MOFs directly. Excitation of the Fe oxo-clusters can lead to transfer of an electron from the bridging $O^{2-}$ to $Fe^{III}$ ions, forming $Fe^{II}$, which can facilitate the reduction of $CO_2$. A series of Fe-containing MOFs, MIL-101(Fe), MIL-53(Fe) and MIL-88B(Fe), have been reported as photocatalysts for reduction of gaseous $CO_2$ to formate in the presence of triethanolamine (TEOA) as a sacrificial electron donor.[159] Each of these MOFs contains the linker $BDC^{2-}$, however the structures of the MOFs differ (Fig. 14). The structure of MIL-53(Fe) is composed of chains of vertex-sharing, hydroxo-bridged $Fe^{III}$ octahedra, which are connected by $BDC^{2-}$ linkers. In contrast, both MIL-88B(Fe) and MIL-101(Fe) have oxo-centred $\{Fe^{III}_3(\mu_3\text{-}O)\}^{7+}$ SBUs. In MIL-88B(Fe), $BDC^{2-}$ linkers connect $Fe_3O$ units to form a porous three-dimensional framework with microporous channels. However, the structure of MIL-101(Fe) contains mesoporous cages.

These structural differences lead to different catalytic activities for each material.[159] The best activity for photocatalytic reduction of $CO_2$ was recorded in MIL-101(Fe), due to the presence of a labile water molecule, which, when removed, leads to an unsaturated coordination site, allowing direct chemical adsorption of $CO_2$ onto the metal centre. Direct adsorption of $CO_2$ at the Fe sites was not observed for MIL-88B(Fe) or MIL-53(Fe). The difference in activity between these three MOFs shows the effect of the inorganic SBU structure on the photocatalytic activity of MOFs.

Further, modification of the organic linker can lead to enhancement of the catalytic activity for each of these Fe-containing MOFs. The catalytic activity of each of these three MOFs was enhanced by functionalisation of the $BDC^{2-}$ linker by an amine group, to give three amino-substituted MOFs, $NH_2$MIL-101(Fe), $NH_2$MIL-53(Fe) and $NH_2$MIL-88B(Fe).[159] This improvement in catalytic activity was attributed to two factors. Firstly, the presence of a polar amino functionality increases the interaction with $CO_2$ molecules, leading to enhanced absorption capacity. Additionally, the amino group enables the absorption of visible light, thus providing an additional pathway for the excitation of the Fe oxo-cluster through energy transfer from the excited ligand. The ability to tune the photocatalytic activity of MOFs by linker and node modification demonstrates the advantage MOFs can provide as molecularly-tunable catalytically active scaffolds.

Amine-functionalised Ti-based MOFs have also been reported as promising photocatalysts for $CO_2$ reduction. For example, Li and co-workers have reported that introduction of an amine group on to the $BDC^{2-}$ ligand in a previously reported titanium-based MOF with octanuclear Ti units, MIL-125,[163] gave the isostructural MOF $NH_2$-MIL-125.[164] Under visible light irradiation, $NH_2$-MIL-125 can reduce $CO_2$ to formate. This photocatalytic activity was not observed in the unfunctionalized MIL-125 MOF under the same conditions.

MOFs have been explored as catalysts for selective reduction of $CO_2$ to CO. For example, Lu and co-workers have reported a MOF which utilises visible light to reduce $CO_2$ to syngas,[165] a mixture consisting primarily of CO and $H_2$, which is used in a diverse range of industrial reactions for the synthesis of hydrocarbons, ammonia for fertiliser production and methanol.[166] Current industrial methods of producing syngas rely on fossil fuel sources. Hence, photocatalytic reduction of $CO_2$ offers a potentially sustainable method of producing syngas under mild conditions. Lu and co-workers designed a photoactive MOF, $(Co/Ru)_{2.4}$-UiO-67(bpydc).[165] The photoactive MOF, $(Co/Ru)_{2.4}$-UiO-67(bpydc), was synthesised by functionalising the Zr-based UiO-67(bpydc) structure with a $Ru^{II}$-based photosensitiser, and a $Co^{II}$ single site catalyst (Fig. 15), whereby the Co:Ru ratio was controlled during the synthesis. In a saturated solution of $CO_2$ in $CH_3CN$ and $H_2O$, containing TEAO as an electron donor, $(Co/Ru)_{2.4}$-UiO-67(bpydc) produced both CO, by reduction of $CO_2$, and $H_2$, by $H_2O$ reduction, when irradiated by visible light (Fig. 15). The syngas yield obtained was 13,600 μmol $g^{-1}$, which was 29.2 times higher than that obtained using the corresponding homogenous system. The relative composition of the CO:$H_2$ mixture was influenced by variation of the $H_2O$ content of the solvent system. Furthermore, systematically varying the Co:Ru ratio in the MOF allowed the CO:$H_2$ product ratio to be varied, thus rendering this MOF system a tunable photocatalyst for syngas production.

### 4.2. Photocatalytic water splitting

Using solar energy to carry out photocatalytic water splitting to produce $H_2$ and $O_2$ is a promising energy conversion and storage approach, providing a potentially sustainable alternative energy source to replace fossil fuels. The advantage that $H_2$ fuel sources possess over fossil fuels is that no emissions are generated from using $H_2$ as fuel.[167] Applications are severely hampered by the high production costs and lack of $H_2$ storage solutions for automotive and transport applications. Electrolysis of water is an energetically uphill process, and research is rapidly progressing to find catalysts for the two half reactions in $H_2O$ splitting, the oxygen evolution reaction (OER) (Reaction 1, Scheme 1) and the hydrogen evolution reaction (HER) (Reaction 2, Scheme 1).[168] A major challenge is developing catalysts for the highly endergonic OER reaction, as the potential required for each electron transferred at pH 0 is 1.23 eV versus NHE (NHE = normal hydrogen electrode).

To design efficient $H_2O$ oxidation catalysts, research activities may take inspiration from the oxygen-evolving complex (OEC) of photosystem II. From a molecular point of view, the 4-electron $H_2O$ oxidation half-equation, coupled to a transfer of 4 protons and the formation of an O-O bond, is one of the most challenging catalytic transformations, and insights into this process can guide the development of highly efficient oxidation catalysts. The complexity and energy demand of this reaction is illustrated by large

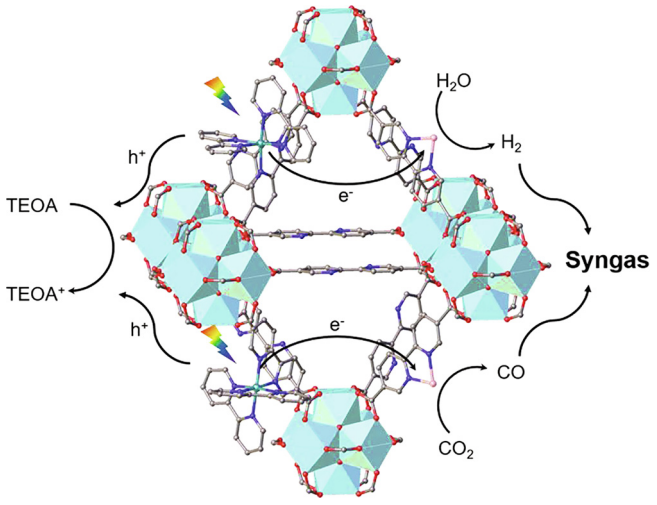


**Fig. 15.** Proposed mechanism of the photocatalytic syngas production by $(Co/Ru)_{2.4}$-UiO-67(bpydc). Directional movements of electrons ($e^-$) and holes ($h^+$) are indicated by arrows (TEOA: triethanolamine).[165]

$$2H_2O \rightarrow O_2 + 4H^+ + 4e^- \qquad E^0 = -1.23\ eV\ (1)$$

$$4H^+ + 4e^- \rightarrow 2H_2 \qquad E^0 = 0.00\ eV\ (2)$$

**Scheme 1.** Half reactions for water splitting, and their respective standard potentials at pH 0 versus NHE.

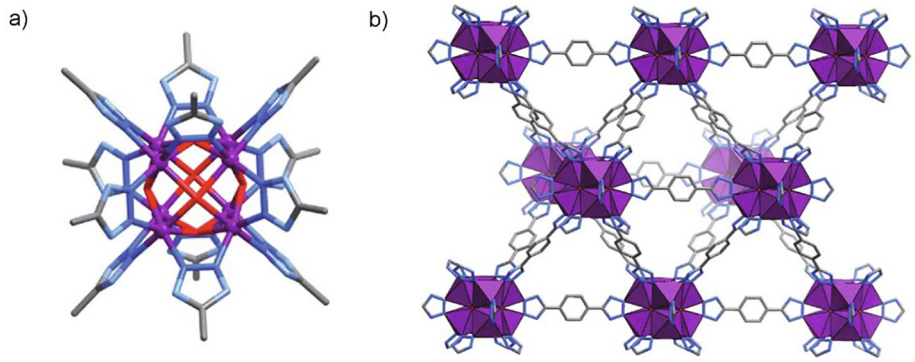


**Fig. 16. a)** SBU of MAF, showing $\{Co^{II}_8(\mu_4\text{-}OH)_6\}$ cluster. **b)** Structure of MAF-48. Reproduced with permission from Ref. [176]. Copyright 2019, The Royal Society of Chemistry.

overpotentials associated with the individual reaction steps. Thus, an energetically favoured catalysed pathway relies on concerted processes in which the substrate and catalyst adopt geometrically constrained conformations. Whilst artificial photosynthetic systems are severely hampered by a lack of active catalysts, nature uses a $\{Mn_4CaO_5\}$ oxo-cluster to oxidize water at efficiencies far exceeding those of any synthetic system. Recent X-ray, spectroscopic and computational studies resulted in new mechanistic insights into the oxidation process.[169–172] Active synthetic molecular oxidation catalysts that relate or mimic the naturally occurring process should be compatible with processes of the Kok cycle,[173] and enable multiple electron transfer (ET) or proton-coupled processes within a narrow potential range. In addition, they should be composed of abundant elements and should be amenable to structural modifications which allow them to interface with sensitisers.

MOFs have been explored as photocatalysts for $H_2O$ splitting due to their tunable photoactivity, large surface areas, favourable diffusion coefficients and high density of active sites per volume, as previously indicated.[31,174] The SBUs of MOFs can incorporate active sites for catalysis, including open metal sites, which have labile coordinating solvent molecules that can be exchanged for substrates during catalytic reactions.[175] The fundamental requirement of such labile coordination sites is exemplified in highly efficient biological or bio-inspired oxidation catalysts including dioxygenases, catalases or the oxygen-evolving complex of photosystem II. In addition, dynamic structures and multiple conformations that are typical for MOFs are widely recognised to be key characteristics, responsible for the performances of biocatalysts. MOFs may impart the principal advantages of heterogeneous catalysts compared to corresponding homogeneous phases, whereby enhanced stability or facile processability in photochemical systems can potentially lead to unique materials.

Cobalt-based MOFs have been reported as effective heterogeneous catalysts for light-driven water oxidation. In 2019, Chen and co-workers reported the synthesis of MAF-48 (MAF = metal-azolate framework), a cobalt-based MOF with the formula $[Co_8(OH)_6(BDT)_4(HBDT)_2]$ ($H_2BDT$ = 1,4-benzenedi(1*H*-1,2,3-triazole)), which functions as a stable heterogenous catalyst for water oxidation.[176] The structure of MAF-48 consists of octanuclear hydroxide-bridged $\{Co^{II}_8(\mu_4\text{-}OH)_6\}$ SBUs, linked by BDT linkers (Fig. 16). Each face of the octanuclear cobalt cluster features four coplanar $Co^{II}$ ions, coordinated to hydroxide ions which adopt $\mu_4$-bridging modes. In the presence of a photosensitiser, $[Ru(bpy)_3]SO_4$, and a sacrificial electron acceptor, $Na_2S_2O_8$, MAF-48 demonstrates photodriven water oxidation when irradiated with visible light. A TOF of 3.05 $s^{-1}$ and a TON of 1.2 $\times$ $10^6$ were recorded, demonstrating the high catalytic activity of MAF-48. In fact, this MOF demonstrates the highest activity of any heterogenous catalyst, except for photosystem II. This study demonstrates the influence of specific SBUs on the activity of MOFs as photocatalysts, as the high activity of MAF-48 was attributed to the structure of the octanuclear $Co^{II}$ hydroxo-cluster. The presence of four $Co^{II}$ ions that coordinate to a central $\mu_4$-$OH^-$ hydroxo ligand leads to a stabilising effect on the reacting hydroxyl radical during the water oxidation cycle, thus enhancing the activity of the MOF.

Due to their ability to absorb visible light, porphyrins represent promising ligands for designing photocatalytic MOFs. For example, the MOF Ru-TBP ($TBP^{4-}$ = 5,10,15,20- tetra(*p*-benzoate)porphyrin) and its zinc-metallated analogue, Ru-TBP-Zn, have been shown to be effective at photochemical evolution of $H_2$.[177] Ru-TBP-Zn was a better photocatalyst than Ru-TBP or $TBP^{4-}$ alone. The MOF is constructed from dinuclear $\{Ru^{II}_2\}$ paddlewheel SBUs linked by tetratopic porphyrin linkers. The mechanism for $H_2$ evolution involved photochemical excitation of the TBP-Zn linker, and subsequent electron transfer to the $\{Ru^{II}_2\}$ SBU. The electrons transferred to the paddlewheel SBU consequently drive the proton reduction to generate $H_2$.

While the reported MAF-48 system utilises $[Ru(bpy)_3]^{2+}$ as a photosensitiser,[176] various different photosensitising ligands can be incorporated into the framework structures. For example, Lin and co-workers recently reported photocatalytic proton or $CO_2$ reduction using a series of MOFs composed of photosensitising $Cu^I$ metalloligands (Fig. 17).[54] Two different post-synthetic modification approaches were applied to obtain functional MOFs, which are *iso*-reticular to UiO-69 and comprise of inorganic $\{Zr_6(\mu_3\text{-}O)_4(\mu_3\text{-}OH)_4\}$ SBUs, that are connected by *p*-phenanthroline dibenzoate (PT) and 4,4′-bis(carboxyphenyl)-2-nitro-1,1′-biphenyl ($CPNBP^{2-}$) moieties.

In the initial study, [55] both the $Cu^I$-based photosensitiser (Cu-PS) as well as the catalytically active site ($Re^I$ or $Co^{II}$ for $CO_2$ or $H^+$ reduction, respectively) were sequentially introduced at the PT ligands, yielding mPT-Cu/Re (Fig. 17b)) and mPT-Cu/Co (Fig. 17c)). In a follow-up study, [54] FeX@mPT-Cu (X = Br, Cl, OAc, $BF_4$) were obtained by sequential instalment of the Cu-PS at the PT-ligands (Fig. 17f)), followed by the introduction of catalytic centres at the inert SBUs through treatment with $Fe^{II}$ salts (Fig. 17g)). In all cases, the photocatalytic cycle is initiated by photoexcitation of Cu-PS to [Cu-PS]*, followed by a reductive quenching pathway, yielding $[Cu\text{-}PS]^-$ and the oxidized sacrificial electron donor (1,3-dimethyl-2-phenyl-2,3-dihydro-1*H*-benzo[*d*]imidazole). Electron transfer from $[Cu\text{-}PS]^-$ to the catalytic centre initiates the reductive transformation of the chosen substrate. The spatial proximity of the components in the MOF as well as the stabilising effect of the framework structure, enhances the catalytic activity in comparison to the corresponding homogeneous phases. When compared to the Cu-PS and $Re^I$- or $Co^{II}$-catalysts in solution, mPT-Cu/Re and mPT-Cu/Co exhibit enhanced catalytic activity by

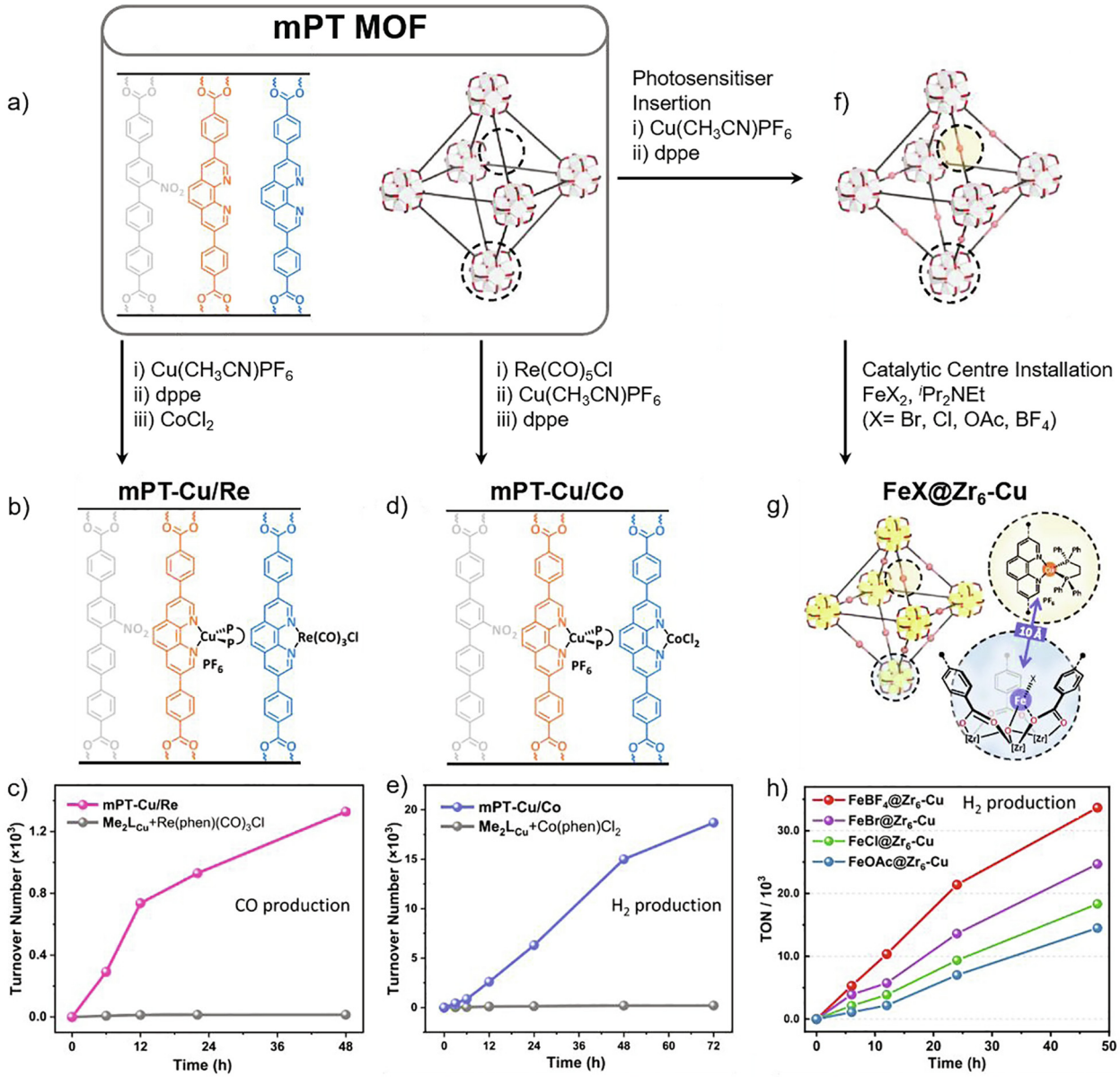


**Fig. 17. a)** Schematic representation of mPT-MOF **b)** Post-synthetic modification of mPT-MOF, giving mPT-Cu/Re (dppe = 1,2-bis(diphenyl-phosphino)ethane) **c)** Time dependent $CO_2$ reduction reaction TONs of mPT-Cu/Re, compared to the homogeneous control experiment **d)** Post-synthetic modification of mPT-MOF, giving mPT-Cu/Co **e)** Time dependent HER TONs of mPT-Cu/Co, compared to the homogeneous control experiment **f)** Installation of $Cu^{I}$ photosensitisers in mPT-MOF **g)** Incorporation of $Fe^{II}$ catalytic centres, giving FeX@$Zr_6$Cu (X = Br, Cl, OAc, $BF_4$) **h)** Time-dependent $H_2$ evolution TONs of FeX@$Zr_6$Cu (X = Br, Cl, OAc, $BF_4$). Adapted with permission from Ref. [54] and Ref. [55]. Copyright 2020, American Chemical Society.

almost two orders of magnitude, with respective $CO_2$ reduction reaction and HER TONs of 1328 and 18,700 (Fig. 17c) and e)). The latter is exceeded further by FeX@mPT-Cu, which display HER TONs of up to 33,700 for $FeBF_4$@$Zr_6$-Cu (Fig. 17h)). Further, it was found that the activity of FeX@mPT-Cu is dependent on the coordination strength of the charge-balancing $X^-$ ion to the $Fe^{II}$ centre, with the weakest coordination resulting in the highest catalytic activity.

Encapsulation of catalytically active guests into the pores of MOFs can enhance their performance of as photocatalysts for water splitting. For example, Kögerler and co-workers reported the encapsulation of two Co-based POMs into a MIL-100 (Fe) MOF,[178] an $Fe^{III}$ carboxylate MOF.[179] The two POMs encapsulated in the MOF, $[Co^{II}Co^{III}W_{11}O_{39}(H_2O)]^{7-}$ (Co2) and $[Co_4(PW_9O_{34})_2(H_2O)_2]^{10-}$ (Co4) had previously been reported to display excellent activities as homogenous catalysts for water oxidation. [180,181] The water oxidation activities of the two composite materials Co2@MIL-100 (Fe) and Co4@MIL-100 (Fe) were studied at pH = 9 and 8 respectively, using $NaS_2O_8$ as a sacrificial electron donor and $Ru(bpy)_3^{2+}$ as a photosensitiser (Fig. 18). Both POMs demonstrated higher catalytic activity when encapsulated into the MOF structure, compared to the POM alone, due to cooperative electrostatic interactions between the MOF and the POM guest. Furthermore, the activity of the catalysts did not significantly decrease when the catalyst was recycled, as the POMs did not leach from the host framework.

Lin and co-workers encapsulated a Wells-Dawson type POM, $[P_2W_{18}O_{62}]^{6-}$, into the pores of a $[Ru(bpy)_3]^{2+}$-derived UiO-type MOF.[182] Visible light irradiation leads to excitation of the Ru-based ligands to the $^1$MLCT excited state, followed by intersystem crossing to the $^3$MLCT state. Subsequent multielectron transfer from the excited metallo-ligand to the encapsulated POMs

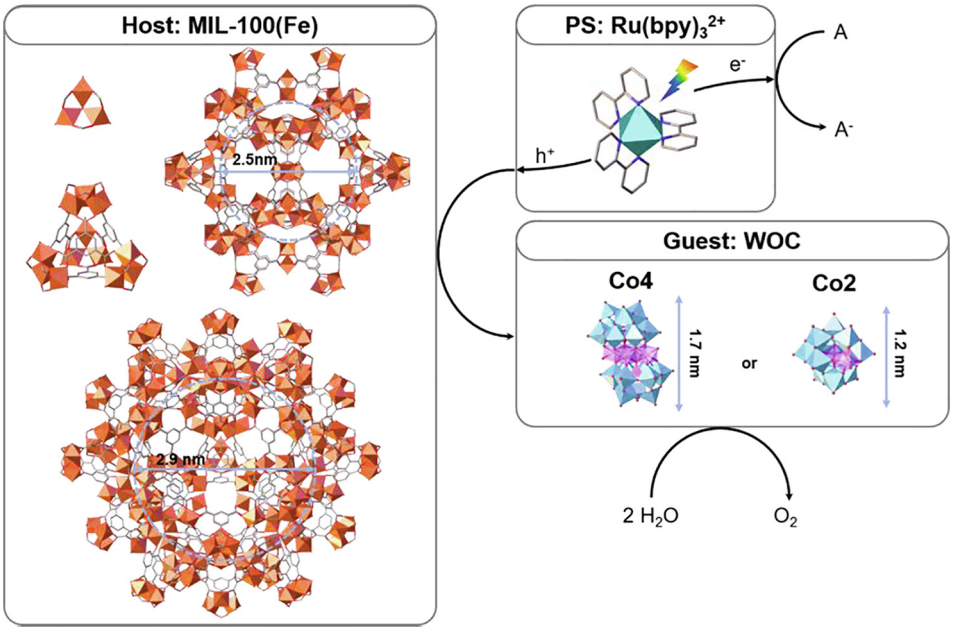


**Fig. 18.** Schematic representation of photocatalytic water oxidation by composite materials Co2@MIL-100 (Fe) and Co4@MIL-100 (Fe).[178]

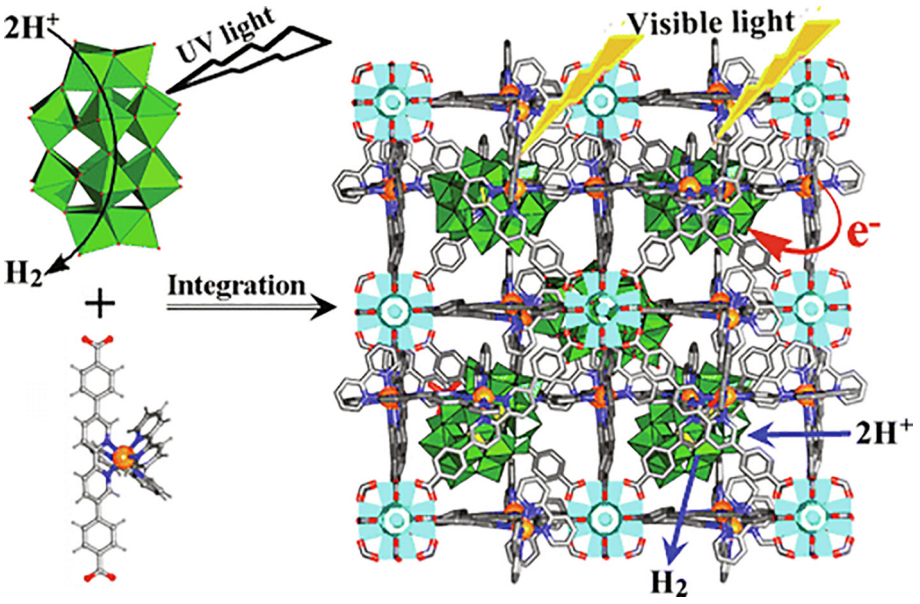


**Fig. 19.** Schematic representation of the mechanism of visible-light-driven proton reduction by the POM@UiO system. Reproduced with permission from Ref. [182]. Copyright 2015, American Chemical Society.

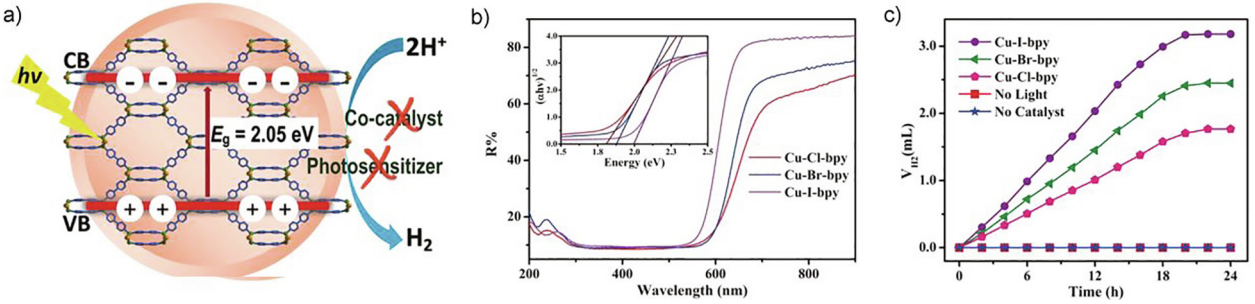


**Fig. 20. a)** Semiconductive MOFs Cu-X-4,4′-bpy as photocatalysts for $H_2$ evolution. **b)** Reflectance spectra and Tauc plot shown in the inset. **c)** Photocatalytic hydrogen evolution in aqueous TEOA (5% v/v, pH 11.5) under UV light irradiation. Reproduced with permission from Ref. [183]. Copyright 2017, Wiley-VCH Verlag GmbH & Co. KGaA, Weinheim.

facilitates the latter to act as a proton reduction catalyst (Fig. 19). A series of POM@UiO materials were synthesised by variation of the quantity of POM in the reaction mixture, yielding highest activity at low POM loading. The materials were recycled thrice with only a minor loss of activity.

Incorporation of functional groups can also enhance the photocatalytic $H_2$ evolution activity of MOFs. For example, introducing a methylthio group (-$SCH_3$) onto the $BDC^{2-}$ linker of MIL-125 gave a MOF which was highly active for light driven $H_2$ evolution.[35] Direct synthesis of MIL-125 with the methylthio-functionalised $BDC^{2-}$ (BDC-$(SCH_3)_2^{2-}$) linker was unsuccessful, and therefore the methylthio-functionalised MOF was synthesised by solvent-assisted ligand-exchange of BDC-$(SCH_3)_2^{2-}$ into the structure of MIL-125. The resulting MOFs, 20%-MIL-125-$(CH_3)_2$, containing 20% BDC-$(SCH_3)_2^{2-}$ and 50%-MIL-125-$(CH_3)_2$, containing BDC-$(SCH_3)_2^{2-}$ showed visible light absorption and lower band gaps of 2.69 eV and 2.61 eV respectively, than that of MIL-125, which has a band gap of 3.8 eV. Additionally, in the presence of Pt as a co-catalyst, and TEOA as a sacrificial electron donor, the MOFs perform well as catalysts for $H_2$ evolution from water. The highest $H_2$ evolution activity was observed for Pt/20%-MIL-125-$(SCH_3)_2$ which had a $H_2$ evolution rate of 3814.0 μmol $g^{-1}h^{-1}$. The enhanced ability of Pt/20%-MIL-125-$(SCH_3)_2$ over Pt/50%-MIL-125-$(SCH_3)_2$ was attributed to the higher stability of Pt/20%-MIL-125-$(SCH_3)_2$.

Recently, the groups of Liu and Du reported that MOFs $[Cu_2X_2(4,4'\text{-bpy})_2]$ (X = Cl, Br, I, 4,4′-bpy = 4,4′-bipyridine) denoted as Cu-X-4,4′-bpy,[183] whose basic structure had been known for 20 years prior,[184,185] are in fact semiconductors with narrow optical band gaps ranging from 1.85 eV for Cu-Cl-4,4′-bpy to 2.00 eV for Cu-I-4,4′bpy (Fig. 20). In these systems, the $\{Cu_2^I(\mu_2\text{-}X)_2\}$ units are linked by four 4,4′-bpy ligands, resulting in orthogonally interpenetrating layers of (3,6)-connected honeycomb nets. Importantly, the Cu-X-4,4′bpy MOFs that self-assemble from inexpensive reagents, were found to be hydrogen evolution photocatalysts. The MOFs operate with visible light irradiation, without requiring any additional photosensitisers or co-catalysts. Particularly high activity and recyclability was demonstrated for Cu-I-4,4′-bpy using TEOA as a sacrificial electron donor.

### 4.3. Degradation of organic pollutants

Organic dyes, in addition to other pollutants, are the by-product of many industrial processes, and many are toxic to humans and to plant and animal life.[186,187] The ability to degrade organic pollutants into less toxic or even harmless compounds is essential for wastewater treatment technologies. MOFs can be designed to photocatalytically degrade organic dyes under various different conditions, including using samples of contaminated wastewater.[188]

In 2016, Zhang and co-workers reported that MIL-53(Fe) could be used as a heterogeneous catalyst containing earth-abundant metal ions for the photochemical degradation of the organic dye Acid Orange 7 (AO7) under visible light irradiation.[189] The catalytic activity originates from charge separated sites which form upon photoexcitation of the structure. However, the catalytic performance of MIL-53(Fe) was hindered by fast recombination of electron-hole pairs after excitation. This deficiency could be overcome by addition of an electron acceptor, sodium persulfate, which was necessary in order to prevent electron-hole recombination, thus enhancing the catalytic activity of the system. In the presence of persulfate, MIL53(Fe) could effectively decolourise a 0.05 mM aqueous solution of AO7 within 90 min of irradiation with a visible light LED (Fig. 21). No substantial difference in activity was recorded after five successive cycles of photocatalytic AO7 degradation, demonstrating that MIL-53(Fe) is a stable and reusable catalyst.

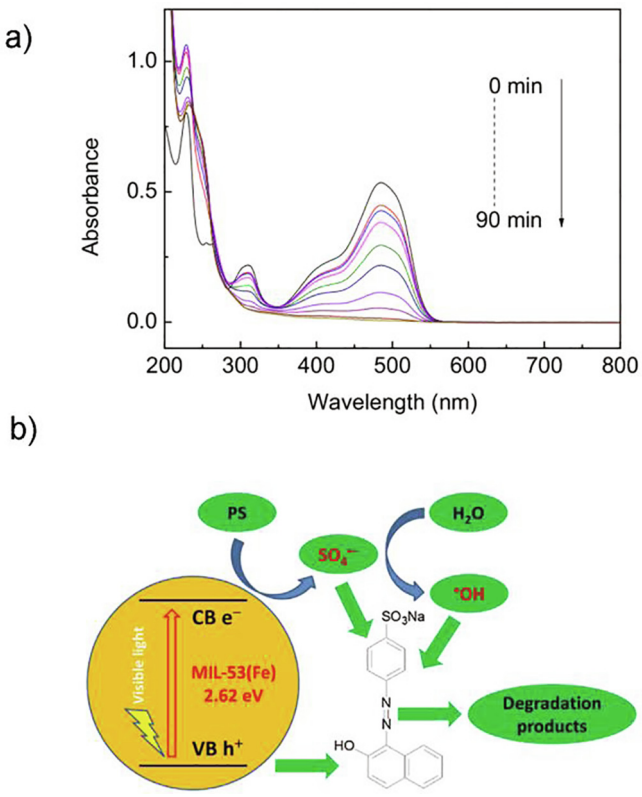


**Fig. 21. a)** Changes in UV-vis spectum during AO7 decolorization by the MIL-53 (Fe)/persulfate/visible light process under the following reaction conditions: AO7 (0.05 mM); MIL-53(Fe) (0.6 g $L^{-1}$); PS = persulfate (2.0 mM); initial pH 6.0. **b)** Mechanism proposed for photocatalytic AO7 degradation by MIL-53(Fe). Reproduced with permission from Ref. [189]. Copyright 2016, Elsevier B.V.

MOF thin films have also been reported as effective photocatalysts for photocatalytic waste treatment. A manganese-based MOF film composed of metalloporphyrin linkers was reported by Zhao and co-workers.[190] The MOF, which is constructed from the metalloporphyrin [5,10,15,20-tetra(4-carboxyphenyl)porphyrin]M $n^{III}$, 2,2′-dimethyl-4,4′-bipyridine (4,4′-DMBP) and zinc acetate, was synthesised by layer-by-layer deposition onto a quartz glass substrate. The structure of the MOF consists of sheets of dinuclear $\{Zn_2^{II}\}$ SBUs connected by the tetratopic metalloporphyrin linker. The layers form parallel to the quartz substrate, and consecutive layers are linked by 4,4′-DMBP pillars. The MOF film was applied to the photocatalytic degradation of an aqueous solution of methylene blue with $H_2O_2$ under irradiation with visible light (400 – 700 nm). The MOF is stable, and can be recycled by washing and drying, and still performs as an effective catalyst after 5 catalytic cycles.

MOFs can also be employed in using visible light for photocatalytic degradation of antibiotics in aqueous solutions. Pollution of water systems by antibiotics can occur due to treatment of livestock with antibiotics.[191] As the incidence of antibiotic resistance increases,[192] the need to treat wastewater to remove antibiotics is vitally important. A europium-based MOF, with the formula $[(CH_3)_2NH_2]_2[Eu_6(OH)_8(ADBA)_6(H_2O)_6]\cdot(DMF)_{15}$ ($H_2$-ADBA = 4,4′-(9,10-anthracenediyl)dibenzoic acid), abbreviated as Eu-ADBA, has been reported to be effective in using visible light to catalyse photodegradation of the antibiotic tetracycline.[193] The linker in this MOF was chosen for the interesting optical attributes of its conjugated anthracene moiety. Eu-ADBA was capable of absorbing organic molecules into the MOF structure and using visible light to catalyse the degradation of two organic dyes, methylene blue and rhodamine B, and tetracycline in water.

## 5. Conclusion

In recent years, MOFs have been explored as promising materials for a wide range of applications, some of which centre on their performance as photoactive materials. Here, characteristics of selected photoactive MOFs have been highlighted considering two broad areas, MOFs as luminescent materials, and photocatalytic MOFs.

The design principles of MOFs, that take advantage of self-assembly approaches and which are governed by the geometrical considerations of their sub-components, impart a degree of synthetic control which is somewhat rare within the area of synthetic materials science. The hybrid nature of the systems results in structural and physico-chemical amenability through both their organic and inorganic building units. Further, the porosity of MOFs often facilitates an extended interface enabling reversible interactions with analytes, substrates or other functionalising molecules which can locate in the cavities. The influence of these tenable features of MOFs are highlighted by the selected examples demonstrating how optical and electronic attributes can be influenced. Of particular note are emerging lanthanide-based MOFs or MOFs containing highly luminescent organic moieties. Through strategic selection of components, MOFs have been reported to be efficient and reusable sensors for a wide range of analytes.

The underlying design principles allow for the preparation of complex photocatalytic systems, that incorporate efficient molecular catalysts within extended frameworks and that operate in the heterogeneous phase. Some prominent examples have the potential to function as artificial photosynthetic systems, using synergistic effects between photosensitisers, catalysts and sacrificial electron donor/acceptors and which find inspiration from biological systems. The extended systems can lead to charge separations whereby a coordination cluster entity can accumulate oxidation/reduction equivalents. The network structures generally enable the required charge transport characteristics, whilst deactivations arising from hydrolytic and oxidative degradation require further investigation. In general, MOFs have shown promising turnover characteristics as photocatalysts in energy conversion/storage systems that promote $H_2O$ splitting to form $O_2$ and $H_2$ or $CO_2$ reduction. These and other examples point towards intriguing future areas of study and potential applications of photoactive MOFs.

## Declaration of Competing Interest

The authors declare that they have no known competing financial interests or personal relationships that could have appeared to influence the work reported in this paper.

## Acknowledgement

The authors gratefully acknowledge the Science Foundation, Ireland (13/IA/1896 and 13/IA/1865), the European Research Council (SUPRAMOL - CoG 2014-647719) and the SFI AMBER and SSPC Research Centres for financial support.

## Appendix A. Supplementary data

Supplementary data to this article can be found online at https://doi.org/10.1016/j.ccr.2020.213757.

## References

[1] S.R. Batten, N.R. Champness, X.-M. Chen, J. Garcia-Martinez, S. Kitagawa, L. Öhrström, M. O'Keeffe, M. Paik, Suh J. Reedijk, Terminology of metal–organic frameworks and coordination polymers (IUPAC Recommendations 2013), Pure Appl. Chem. 85 (2013) 1715–1724, https://doi.org/10.1351/PAC-REC-12-11-20.

[2] A.C. Sudik, A.R. Millward, N.W. Ockwig, A.P. Côté, J. Kim, O.M. Yaghi, Design, synthesis, structure, and gas ($N_2$, Ar, $CO_2$, $CH_4$, and $H_2$) sorption properties of porous metal-organic tetrahedral and heterocuboidal polyhedra, J. Am. Chem. Soc. 127 (19) (2005) 7110–7118, https://doi.org/10.1021/ja042802q.

[3] S. Subramanian, M.J. Zaworotko, Porous solids by design:[Zn(4,4′-bpy)$_2$(SiF$_6$)]$_n$·xDMF, a single framework octahedral coordination polymer with large square channels, Angew. Chem. Int. Ed. Engl. 34 (19) (1995) 2127–2129, https://doi.org/10.1002/anie.199521271.

[4] B.F. Hoskins, R. Robson, Design and construction of a new class of scaffolding-like materials comprising infinite polymeric frameworks of 3D-linked molecular rods. A reappraisal of the $Zn(CN)_2$ and $Cd(CN)_2$ structures and the synthesis and structure of the diamond-related frameworks [$N(CH3)_4$][CuIZnII($CN)_4$] and CuI[4,4"4",4"'-tetracyanotetraphenylmethane]BF4·xC6H5NO2, J. Am. Chem. Soc. 112 (1990) 1546–1554.

[5] B.F. Abrahams, B.F. Hoskins, D.M. Michail, R. Robson, Assembly of porphyrin building blocks into network structures with large channels, Nature 369 (6483) (1994) 727–729, https://doi.org/10.1038/369727a0.

[6] M. Munakata, L.P. Wu, T. Kuroda-Sowa, M. Maekawa, K. Moriwaki, S. Kitagawa, Two types of new polymeric Copper(I) complexes of pyrazinecarboxamide having channel and helical structures, Inorg. Chem. 36 (23) (1997) 5416–5418, https://doi.org/10.1021/ic970427f.

[7] D.-L. Long, A.J. Blake, N.R. Champness, M. Schröder, Lanthanide co-ordination frameworks of 4,4′-bipyridine-N,N′-dioxide, Chem. Commun. (2000) 1369–1370, https://doi.org/10.1039/b002363i.

[8] B. Chen, S. Ma, F. Zapata, F.R. Fronczek, E.B. Lobkovsky, H.-C. Zhou, Rationally designed micropores within a metal−organic framework for selective sorption of gas molecules, Inorg. Chem. 46 (4) (2007) 1233–1236, https://doi.org/10.1021/ic0616434.

[9] C. Livage, N. Guillou, Jérôme Marrot, Gérard Férey, Construction of two- and three-dimensional coordination polymers from cobalt trimesate, Chem. Mater. 13 (11) (2001) 4387–4392, https://doi.org/10.1021/cm011115k.

[10] O.M. Yaghi, M. O'Keeffe, N.W. Ockwig, H.K. Chae, M. Eddaoudi, J. Kim, Reticular synthesis and the design of new materials, Nature 423 (6941) (2003) 705–714, https://doi.org/10.1038/nature01650.

[11] J.V. Smith, Topochemistry of zeolites and related materials. 1. Topology and geometry, Chem. Rev. 88 (1) (1988) 149–182, https://doi.org/10.1021/cr00083a008.

[12] D.W. Breck, Zeolite Molecular Sieves: Structure, Chemistry, and Use, John Wiley & Sons, New York, 1973.

[13] J. Kim, B. Chen, T.M. Reineke, H. Li, M. Eddaoudi, D.B. Moler, M. O'Keeffe, O.M. Yaghi, Assembly of Metal−Organic Frameworks from Large Organic and Inorganic Secondary Building Units: New Examples and Simplifying Principles for Complex Structures, J. Am. Chem. Soc. 123 (2001) 8239–8247, https://doi.org/10.1021/ja010825o.

[14] V.A. Blatov, M. O'Keeffe, D.M. Proserpio, Vertex-, face-, point-, Schläfli-, and Delaney-symbols in nets, polyhedra and tilings: recommended terminology, CrystEngComm 12 (1) (2010) 44–48, https://doi.org/10.1039/B910671E.

[15] M. O'Keeffe, M.A. Peskov, S.J. Ramsden, O.M. Yaghi, The reticular chemistry structure resource (RCSR) database of, and symbols for, crystal nets, Acc. Chem. Res. 41 (12) (2008) 1782–1789, https://doi.org/10.1021/ar800124u.

[16] S. Jeoung, S. Kim, M. Kim, H.R. Moon, Pore engineering of metal-organic frameworks with coordinating functionalities, Coordinat. Chem. Rev. 420 (2020) 213377, https://doi.org/10.1016/j.ccr.2020.213377.

[17] D. Aulakh, T. Islamoglu, V.F. Bagundes, J.R. Varghese, K. Duell, M. Joy, S.J. Teat, O.K. Farha, M. Wriedt, Rational Design of Pore Size and Functionality in a Series of Isoreticular Zwitterionic Metal–Organic Frameworks, Chem. Mater. 30 (22) (2018) 8332–8342, https://doi.org/10.1021/acs.chemmater.8b03885.

[18] M.-H. Zeng, Q.-X. Wang, Y.-X. Tan, S. Hu, H.-X. Zhao, L.-S. Long, M. Kurmoo, Rigid Pillars and Double Walls in a Porous Metal-Organic Framework: Single-Crystal to Single-Crystal, Controlled Uptake and Release of Iodine and Electrical Conductivity, J. Am. Chem. Soc. 132 (8) (2010) 2561–2563, https://doi.org/10.1021/ja908293n.

[19] F. Chen, Y.-M. Wang, W. Guo, X.-B. Yin, Color-tunable lanthanide metal–organic framework gels, Chem. Sci. 10 (6) (2019) 1644–1650, https://doi.org/10.1039/C8SC04732D.

[20] M.C. Wasson, C.T. Buru, Z. Chen, T. Islamoglu, O.K. Farha, Metal–organic frameworks: A tunable platform to access single-site heterogeneous catalysts, Appl. Catal. A: Gen. 586 (2019) 117214, https://doi.org/10.1016/j.apcata.2019.117214.

[21] A.M. Ullman, J.W. Brown, M.E. Foster, F. Léonard, K. Leong, V. Stavila, M.D. Allendorf, Transforming MOFs for energy applications using the Guest@MOF concept, Inorg. Chem. 55 (15) (2016) 7233–7249, https://doi.org/10.1021/acs.inorgchem.6b00909.

[22] J.-L. Wang, C. Wang, W. Lin, Metal–Organic Frameworks for Light Harvesting and Photocatalysis, ACS Catal. 2 (12) (2012) 2630–2640, https://doi.org/10.1021/cs3005874.

[23] J. Baek, B. Rungtaweevoranit, X. Pei, M. Park, S.C. Fakra, Y.-S. Liu, R. Matheu, S. A. Alshmimri, S. Alshehri, C.A. Trickett, G.A. Somorjai, O.M. Yaghi, Bioinspired metal–organic framework catalysts for selective methane oxidation to methanol, J. Am. Chem. Soc. 140 (51) (2018) 18208–18216, https://doi.org/10.1021/jacs.8b11525.

[24] Y. Li, H. Xu, S. Ouyang, J. Ye, Metal–organic frameworks for photocatalysis, Phys. Chem. Chem. Phys. 18 (11) (2016) 7563–7572, https://doi.org/10.1039/C5CP05885F.

[25] D. Sensharma, N. Zhu, S. Tandon, S. Vaesen, G.W. Watson, W. Schmitt, Flexible metal–organic frameworks for light-switchable $CO_2$ sorption using an auxiliary ligand strategy, Inorg. Chem. 58 (15) (2019) 9766–9772, https://doi.org/10.1021/acs.inorgchem.9b00768.

[26] P. Vervoorts, A. Schneemann, I. Hante, J. Pirillo, Y. Hijikata, T. Toyao, K. Kon, K.-ichi. Shimizu, T. Nakamura, S.-ichiro. Noro, R.A. Fischer, Coordinated water as new binding sites for the separation of light hydrocarbons in metal–organic frameworks with open metal sites, ACS Appl. Mater. Interfaces 12 (8) (2020) 9448–9456, https://doi.org/10.1021/acsami.9b21261.

[27] B. Chen, C. Liang, J. Yang, D.S. Contreras, Y.L. Clancy, E.B. Lobkovsky, O.M. Yaghi, S. Dai, A microporous metal–organic framework for gas-chromatographic separation of alkanes, Angew. Chem. Int. Ed. 45 (9) (2006) 1390–1393, https://doi.org/10.1002/anie.200502844.

[28] J. Wang, J. Wang, Y. Li, M. Jiang, L. Zhang, P. Wu, A europium(III)-based metal–organic framework as a naked-eye and fast response luminescence sensor for acetone and ferric iron, New J. Chem. 40 (2016) 8600–8606, https://doi.org/10.1039/C6NJ02163H.

[29] M.-L. Gao, X.-M. Cao, Y.-Y. Zhang, M.-H. Qi, S.-M. Wang, L. Liu, Z.-B. Han, A bifunctional luminescent europium–organic framework for highly selective sensing of nitrobenzene and 4-aminophenol, RSC Adv. 7 (71) (2017) 45029–45033, https://doi.org/10.1039/C7RA08885J.

[30] K. Lu, C. He, W. Lin, Nanoscale metal–organic framework for highly effective photodynamic therapy of resistant head and neck cancer, J. Am. Chem. Soc. 136 (48) (2014) 16712–16715, https://doi.org/10.1021/ja508679h.

[31] H. Furukawa, K.E. Cordova, M. O'Keeffe, O.M. Yaghi, The chemistry and applications of metal-organic frameworks, Science 341 (6149) (2013) 1230444, https://doi.org/10.1126/science:1230444.

[32] C.Y. Lee, O.K. Farha, B.J. Hong, A.A. Sarjeant, SonBinh.T. Nguyen, J.T. Hupp, Light-harvesting metal–organic frameworks (MOFs): efficient strut-to-strut energy transfer in bodipy and porphyrin-based MOFs, J. Am. Chem. Soc. 133 (40) (2011) 15858–15861, https://doi.org/10.1021/ja206029a.

[33] E.P. McCarney, C.S. Hawes, J.A. Kitchen, K. Byrne, W. Schmitt, T. Gunnlaugsson, A Lanthanide luminescent cation exchange material derived from a flexible tricarboxylic acid 2,6-Bis(1,2,3-Triazol-4-yl)pyridine (btp) tecton, Inorg. Chem. 57 (2018) 3920–3930, https://doi.org/10.1021/acs.inorgchem.8b00080.

[34] C.-X. Chen, Q.-F. Qiu, M. Pan, C.-C. Cao, N.-X. Zhu, H.-P. Wang, J.-J. Jiang, Z.-W. Wei, C.-Y. Su, Tunability of fluorescent metal–organic frameworks through dynamic spacer installation with multivariate fluorophores, Chem. Commun. 54 (97) (2018) 13666–13669, https://doi.org/10.1039/C8CC07441K.

[35] S.-Y. Han, D.-L. Pan, H. Chen, X.-B. Bu, Y.-X. Gao, H. Gao, Y. Tian, G.-S. Li, G. Wang, S.-L. Cao, C.-Q. Wan, G.-C. Guo, A methylthio-functionalized-MOF photocatalyst with high performance for visible-light-driven $H_2$ evolution, Angew. Chem. Int. Ed. 57 (31) (2018) 9864–9869, https://doi.org/10.1002/anie.201806077.

[36] Z. Wu, X. Huang, H. Zheng, P. Wang, G. Hai, W. Dong, G. Wang, Aromatic heterocycle-grafted $NH_2$-MIL-125(Ti) via conjugated linker with enhanced photocatalytic activity for selective oxidation of alcohols under visible light, Appl. Catal. B: Environ. 224 (2018) 479–487, https://doi.org/10.1016/j.apcatb.2017.10.034.

[37] U.J. Ryu, S.J. Kim, H.-K. Lim, H. Kim, K.M. Choi, J.K. Kang, Synergistic interaction of Re complex and amine functionalized multiple ligands in metal-organic frameworks for conversion of carbon dioxide, Sci Rep 7 (1) (2017), https://doi.org/10.1038/s41598-017-00574-1.

[38] C.R. McKeithan, L. Wojtas, R.W. Larsen, Guest to framework photoinduced electron transfer in a cobalt substituted RWLC-2 metal organic framework, Dalton Trans. 47 (28) (2018) 9250–9256, https://doi.org/10.1039/C8DT01287C.

[39] K.G.M. Laurier, F. Vermoortele, R. Ameloot, D.E. De Vos, J. Hofkens, M.B.J. Roeffaers, Iron(III)-based metal–organic frameworks as visible light photocatalysts, J. Am. Chem. Soc. 135 (39) (2013) 14488–14491, https://doi.org/10.1021/ja405086e.

[40] C.-K. Lin, D. Zhao, W.-Y. Gao, Z. Yang, J. Ye, T. Xu, Q. Ge, S. Ma, D.-J. Liu, Tunability of Band Gaps in Metal–Organic Frameworks, Inorg. Chem. 51 (16) (2012) 9039–9044, https://doi.org/10.1021/ic301189m.

[41] G. Tobin, S. Comby, N. Zhu, R. Clérac, T. Gunnlaugsson, W. Schmitt, Towards multifunctional lanthanide-based metal–organic frameworks, Chem. Commun. 51 (68) (2015) 13313–13316, https://doi.org/10.1039/C5CC04928H.

[42] C.S. Hawes, Gearóid.M. Ó Máille, K. Byrne, W. Schmitt, T. Gunnlaugsson, Tetraarylpyrrolo[3,2- b ]pyrroles as versatile and responsive fluorescent linkers in metal–organic frameworks, Dalton Trans. 47 (30) (2018) 10080–10092, https://doi.org/10.1039/C8DT01784K.

[43] W. Yin, C.-an. Tao, F. Wang, J. Huang, T. Qu, J. Wang, Tuning optical properties of MOF-based thin films by changing the ligands of MOFs, Sci. China Mater. 61 (3) (2018) 391–400.

[44] E. Flage−Larsen, A. Røyset, J.H. Cavka, K. Thorshaug, Band gap modulations in UiO metal–organic frameworks, J. Phys. Chem. C 117 (40) (2013) 20610–20616, https://doi.org/10.1021/jp405335q.

[45] J.A. Johnson, J. Luo, X. Zhang, Y.-S. Chen, M.D. Morton, E. Echeverría, F.E. Torres, J. Zhang, Porphyrin-Metalation-Mediated Tuning of Photoredox Catalytic Properties in Metal–Organic Frameworks, ACS Catal. 5 (9) (2015) 5283–5291, https://doi.org/10.1021/acscatal.5b00941.

[46] S. Nakagaki, G. Ferreira, G. Ucoski, K. Dias de Freitas Castro, Chemical Reactions Catalyzed by Metalloporphyrin-Based Metal-Organic Frameworks, Molecules. 18 (2013) 7279–7308. Doi: 10.3390/molecules18067279.

[47] C. Pereira, M. Simões, J. Tomé, F. Almeida Paz, Porphyrin-Based Metal-Organic Frameworks as Heterogeneous Catalysts in Oxidation Reactions, Molecules. 21 (2016) 1348. https://doi.org/10.3390/molecules21101348.

[48] J. Weynand, A. Moreno-Betancourt, F. Loiseau, N. Berthet, E. Defrancq, B. Elias, Redox-active bis-cyclometalated iridium(III) complex as a DNA photo-cleaving agent, Inorg. Chem. 59 (4) (2020) 2426–2433, https://doi.org/10.1021/acs.inorgchem.9b03312.

[49] A. Hergueta-Bravo, M.E. Jiménez-Hernández, F. Montero, E. Oliveros, G. Orellana, Singlet oxygen-mediated DNA photocleavage with Ru(II) polypyridyl complexes, J. Phys. Chem. B 106 (15) (2002) 4010–4017, https://doi.org/10.1021/jp013542r.

[50] K. Fan, S.-S. Bao, W.-X. Nie, C.-H. Liao, L.-M. Zheng, Iridium(III)-based metal–organic frameworks as multiresponsive luminescent sensors for $Fe^{3+}$, $Cr_2O_7^{2-}$, and $ATP^{2-}$ in aqueous media, Inorg. Chem. 57 (3) (2018) 1079–1089, https://doi.org/10.1021/acs.inorgchem.7b02513.

[51] A.M. Rasero-Almansa, A. Corma, M. Iglesias, Félix Sánchez, Post-functionalized iridium–Zr-MOF as a promising recyclable catalyst for the hydrogenation of aromatics, Green Chem. 16 (7) (2014) 3522–3527, https://doi.org/10.1039/C4GC00581C.

[52] L. Martins, L.K. Macreadie, D. Sensharma, S. Vaesen, X. Zhang, J.J. Gough, M. O'Doherty, N.-Y. Zhu, M. Rüther, J.E. O'Brien, A.L. Bradley, W. Schmitt, Light-harvesting, 3rd generation $Ru^{II}/Co^{II}$ MOF with a large, tubular channel aperture, Chem. Commun. 55 (34) (2019) 5013–5016, https://doi.org/10.1039/C9CC00206E.

[53] Z.-H. Yan, M.-H. Du, J. Liu, S. Jin, C. Wang, G.-L. Zhuang, X.-J. Kong, L.-S. Long, L.-S. Zheng, Photo-generated dinuclear $\{Eu(II)\}_2$ active sites for selective $CO_2$ reduction in a photosensitizing metal-organic framework, Nat Commun 9 (1) (2018), https://doi.org/10.1038/s41467-018-05659-7.

[54] Y. Pi, X. Feng, Y. Song, Z. Xu, Z. Li, W. Lin, Metal–organic frameworks integrate cu photosensitizers and secondary building unit-supported Fe catalysts for photocatalytic hydrogen evolution, J. Am. Chem. Soc. 142 (23) (2020) 10302–10307, https://doi.org/10.1021/jacs.0c03906.

[55] X. Feng, Y. Pi, Y. Song, C. Brzezinski, Z. Xu, Z. Li, W. Lin, Metal–organic frameworks significantly enhance photocatalytic hydrogen evolution and $CO_2$ reduction with earth-abundant copper photosensitizers, J. Am. Chem. Soc. 142 (2) (2020) 690–695, https://doi.org/10.1021/jacs.9b12229.

[56] C.H. Hendon, D. Tiana, M. Fontecave, C. Sanchez, L. D'arras, C. Sassoye, L. Rozes, C. Mellot-Draznieks, A. Walsh, Engineering the optical response of the titanium-MIL-125 metal–organic framework through ligand functionalization, J. Am. Chem. Soc. 135 (30) (2013) 10942–10945, https://doi.org/10.1021/ja405350u.

[57] J.R. Lakowicz (Ed.), Principles of Fluorescence Spectroscopy, Springer US, Boston, MA, 2006. https://doi.org/10.1007/978-0-387-46312-4.

[58] B. Wardle, Principles and Applications of Photochemistry, John Wiley & Sons, 2009.

[59] J.-C. Bünzli, S.V. Eliseeva, Intriguing aspects of lanthanide luminescence, Chem. Sci. 4 (5) (2013) 1939, https://doi.org/10.1039/c3sc22126a.

[60] J. Soriano-López, D.G. Musaev, C.L. Hill, José.Ramón. Galán-Mascarós, J.J. Carbó, J.M. Poblet, Tetracobalt-polyoxometalate catalysts for water oxidation: Key mechanistic details, J. Catal. 350 (2017) 56–63, https://doi.org/10.1016/j.jcat.2017.03.018.

[61] X. Zhou, B. Li, G. Li, Q. zhou, Z. Shi, S. Feng, Synthesis, structures and luminescent properties of cadmium(ii) metal organic frameworks based on 3-pyrid-4-ylbenzoic acid, 4-pyrid-4-ylbenzoic acid ligands, CrystEngComm 14 (14) (2012) 4664, https://doi.org/10.1039/c2ce25328c.

[62] T.-G. Qu, X.-M. Hao, H. Wang, X.-G. Cui, F. Chen, Y.-B. Wu, D. Yang, M. Zhang, W.-L. Guo, A luminescent 2D zinc(II) metal–organic framework for selective sensing of Fe(III) ions and adsorption of organic dyes, Polyhedron 156 (2018) 208–217, https://doi.org/10.1016/j.poly.2018.09.039.

[63] M.-N. Zhang, T.-T. Fan, Q.-S. Wang, H.-L. Han, X. Li, Zn/Cd/Cu- frameworks constructed by 3,3′-diphenyldicarboxylate and 1,4-bis(1,2,4-triazol-1-yl) butane: Syntheses, structure, luminescence and luminescence sensing for metal ion in aqueous medium, J. Solid State Chem. 258 (2018) 744–752, https://doi.org/10.1016/j.jssc.2017.12.005.

[64] Y.-J. Yang, D. Liu, Y.-H. Li, G.-Y. Dong, Two new luminescent ternary Cd(II)-MOFs by regulation of aromatic dicarboxylate ligands used as efficient dual-responsive sensors for toxic metal ions in water, Polyhedron 159 (2019) 32–42, https://doi.org/10.1016/j.poly.2018.11.051.

[65] G.-X. Wen, Y.-P. Wu, W.-W. Dong, J. Zhao, D.-S. Li, J. Zhang, An ultrastable europium(III)–organic framework with the capacity of discriminating $Fe^{2+}$/$Fe^{3+}$ ions in various solutions, Inorg. Chem. 55 (20) (2016) 10114–10117.

[66] W.T. Carnall, Handbook on the Physics and Chemistry of Rare Earths, Vol. 3, North Holland Publishing Co., Amsterdam, 1979.

[67] J.-C.G. Bünzli, S. V. Eliseeva, Basics of Lanthanide Photophysics, in: Springer Ser. Fluoresc., 2010: pp. 1–45. Doi: 10.1007/4243_2010_3.

[68] J.A. Ridenour, R.G. Surbella III, A.V. Gelis, D. Koury, F. Poineau, K.R. Czerwinski, C.L. Cahill, An americium-containing metal–organic framework: a platform for studying transplutonium elements, Angew. Chem. Int. Ed. 58 (46) (2019) 16508–16511, https://doi.org/10.1002/anie.201909988.

[69] S. Lee, E.A. Kapustin, O.M. Yaghi, Coordinative alignment of molecules in chiral metal-organic frameworks, Science 353 (6301) (2016) 808–811, https://doi.org/10.1126/science.aaf9135.

[70] T.L. Easun, F. Moreau, Y. Yan, S. Yang, M. Schröder, Structural and dynamic studies of substrate binding in porous metal–organic frameworks, Chem. Soc. Rev. 46 (1) (2017) 239–274, https://doi.org/10.1039/C6CS00603E.

[71] M. Müller, A. Devaux, C.-H. Yang, L. De Cola, R.A. Fischer, Highly emissive metal–organic framework composites by host–guest chemistry, Photochem. Photobiol. Sci. 9 (6) (2010) 846, https://doi.org/10.1039/c0pp00070a.

[72] X. Zhao, X. Song, Y. Li, Z. Chang, L. Chen, Targeted construction of light-harvesting metal–organic frameworks featuring efficient host–guest energy transfer, ACS Appl. Mater. Interfaces 10 (6) (2018) 5633–5640, https://doi.org/10.1021/acsami.7b17755.

[73] F. Johnsson, J. Kjärstad, J. Rootzén, The threat to climate change mitigation posed by the abundance of fossil fuels, Climate Policy 19 (2) (2019) 258–274, https://doi.org/10.1080/14693062.2018.1483885.

[74] H. Le Treut, R. Somerville, U. Cubasch, Y. Ding, C. Mauritzen, A. Mokssit, T. Peterson, M. Prather, Historical Overview of Climate Change Science, in: S. Solomon, D. Qin, M. Manning, Z. Chen, M. Marquis, K.B. Averyt, M. Tignor, H.L. Miller (Eds.), Climate Change 2007: The Physical Science Basis. Contribution of Working Group I to the Fourth Assessment Report of the Intergovernmental Panel on Climate Change, Cambridge University Press, Cambridge, United Kingdom and New York, NY, USA, 2007: pp. 95–127.

[75] A.H. Chughtai, N. Ahmad, H.A. Younus, A. Laypkov, F. Verpoort, Metal–organic frameworks: versatile heterogeneous catalysts for efficient catalytic organic transformations, Chem. Soc. Rev. 44 (19) (2015) 6804–6849, https://doi.org/10.1039/c4cs00395k.

[76] J. Liu, L. Chen, H. Cui, J. Zhang, L. Zhang, C.-Y. Su, Applications of metal–organic frameworks in heterogeneous supramolecular catalysis, Chem. Soc. Rev. 43 (16) (2014) 6011–6061, https://doi.org/10.1039/c4cs00094c.

[77] J. Pang, Z. Di, J.-S. Qin, S. Yuan, C.T. Lollar, J. Li, P. Zhang, M. Wu, D. Yuan, M. Hong, H.-C. Zhou, Precisely embedding active sites into a mesoporous zr-framework through linker installation for high-efficiency photocatalysis, J. Am. Chem. Soc. 142 (35) (2020) 15020–15026, https://doi.org/10.1021/jacs.0c05758.

[78] T. Zhang, W. Lin, Metal–organic frameworks for artificial photosynthesis and photocatalysis, Chem. Soc. Rev. 43 (16) (2014) 5982–5993, https://doi.org/10.1039/c4cs00103f.

[79] H.-Q. Xu, J. Hu, D. Wang, Z. Li, Q. Zhang, Y. Luo, S.-H. Yu, H.-L. Jiang, Visible-light photoreduction of $CO_2$ in a metal–organic framework: boosting electron–hole separation via electron trap states, J. Am. Chem. Soc. 137 (42) (2015) 13440–13443, https://doi.org/10.1021/jacs.5b08773.

[80] J.G. Santaclara, F. Kapteijn, J. Gascon, M.A. van der Veen, Understanding metal–organic frameworks for photocatalytic solar fuel production, CrystEngComm 19 (29) (2017) 4118–4125, https://doi.org/10.1039/C7CE00006E.

[81] D. Wu, A.C. Sedgwick, T. Gunnlaugsson, E.U. Akkaya, J. Yoon, T.D. James, Fluorescent chemosensors: the past, present and future, Chem. Soc. Rev. 46 (23) (2017) 7105–7123, https://doi.org/10.1039/c7cs00240h.

[82] J. Zhang, T. Xia, D. Zhao, Y. Cui, Y. Yang, G. Qian, In situ secondary growth of Eu (III)-organic framework film for fluorescence sensing of sulfur dioxide, Sens. Actuat. B: Chem. 260 (2018) 63–69, https://doi.org/10.1016/j.snb.2017.12.187.

[83] J.A. Smith, M.A. Singh-Wilmot, K.P. Carter, C.L. Cahill, J.A. Ridenour, Lanthanide-2,3,5,6-tetrabromoterephthalic acid metal-organic frameworks: evolution of halogen·halogen interactions across the lanthanide series and their potential as selective bifunctional sensors for the detection of $Fe^{3+}$, $Cu^{2+}$, Cryst. Growth Des. 19 (2019) 305–319, https://doi.org/10.1021/acs.cgd.8b01426.

[84] W.-H. Huang, J. Ren, Y.-H. Yang, X.-M. Li, Q. Wang, N. Jiang, J.-Q. Yu, F. Wang, J. Zhang, Water-stable metal–organic frameworks with selective sensing on $Fe^{3+}$ and nitroaromatic explosives, and stimuli-responsive luminescence on lanthanide encapsulation, Inorg. Chem. 58 (2) (2019) 1481–1491, https://doi.org/10.1021/acs.inorgchem.8b02994.

[85] Y.-L. Gai, Q. Guo, X.-Y. Zhao, Y. Chen, S. Liu, Y. Zhang, C.-X. Zhuo, C. Yao, K.-C. Xiong, Extremely stable europium-organic framework for luminescent sensing of $Cr_2O_7^{2-}$ and $Fe^{3+}$ in aqueous systems, Dalton Trans. 47 (35) (2018) 12051–12055, https://doi.org/10.1039/C8DT02313A.

[86] F. Guo, C. Su, Y. Fan, W. Shi, X. Zhang, Construction of a dual-response luminescent metal-organic framework with excellent stability for detecting $Fe^{3+}$ and antibiotic with high selectivity and sensitivity, J. Solid State Chem. 284 (2020) 121183, https://doi.org/10.1016/j.jssc.2020.121183.

[87] Y.-J. Yang, Y.-H. Li, D. Liu, G.-H. Cui, A dual-responsive luminescent sensor based on a water-stable Cd(II)-MOF for the highly selective and sensitive detection of acetylacetone and $Cr_2O_7^{2-}$ in aqueous solutions, CrystEngComm. 22 (2020) 1166–1175, https://doi.org/10.1039/C9CE01546A.

[88] X. Zhang, Z. Zhan, X. Liang, C. Chen, X. Liu, Y. Jia, M. Hu, Lanthanide-MOFs constructed from mixed dicarboxylate ligands as selective multi-responsive luminescent sensors, Dalton Trans. 47 (10) (2018) 3272–3282, https://doi.org/10.1039/C7DT02966G.

[89] N. Xu, Q. Zhang, B. Hou, Q. Cheng, G. Zhang, A novel magnesium metal–organic framework as a multiresponsive luminescent sensor for Fe(III) ions, pesticides, and antibiotics with high selectivity and sensitivity, Inorg. Chem. 57 (21) (2018) 13330–13340, https://doi.org/10.1021/acs.inorgchem.8b01903.

[90] M. Zhang, G. Feng, Z. Song, Y.-P. Zhou, H.-Y. Chao, D. Yuan, T.T.Y. Tan, Z. Guo, Z. Hu, B.Z. Tang, B. Liu, D. Zhao, Two-dimensional metal–organic framework with wide channels and responsive turn-on fluorescence for the chemical sensing of volatile organic compounds, J. Am. Chem. Soc. 136 (20) (2014) 7241–7244, https://doi.org/10.1021/ja502643p.

[91] Y.-Q. Wang, Q.-H. Tan, H.-T. Liu, W. -Sun, Z.-L. Liu, A luminescent europium MOF containing Lewis basic pyridyl site for highly selective sensing of o-, m- and p-nitrophenol, RSC Adv. 5 (105) (2015) 86614–86619, https://doi.org/10.1039/C5RA17001J.

[92] W. Liu, Y. Wang, L. Song, M.A. Silver, J. Xie, L. Zhang, L. Chen, J. Diwu, Z. Chai, S. Wang, Efficient and selective sensing of $Cu^{2+}$ and $UO_2^{2+}$ by a europium metal-organic framework, Talanta 196 (2019) 515–522, https://doi.org/10.1016/j.talanta.2018.12.088.

[93] A. Legrand, A. Pastushenko, V. Lysenko, A. Geloen, E.A. Quadrelli, J. Canivet, D. Farrusseng, Enhanced ligand-based luminescence in metal-organic framework sensor, ChemNanoMat. 2 (9) (2016) 866–872, https://doi.org/10.1002/cnma.201600124.

[94] K. Zheng, Z.-Q. Liu, Y. Huang, F. Chen, C.-H. Zeng, S. Zhong, S.W. Ng, Highly luminescent Ln-MOFs based on 1,3-adamantanediacetic acid as bifunctional sensor, Sens. Actuat. B: Chem. 257 (2018) 705–713, https://doi.org/10.1016/j.snb.2017.11.009.

[95] S. Khatua, S. Goswami, S. Biswas, K. Tomar, H.S. Jena, S. Konar, Stable multiresponsive luminescent MOF for colorimetric detection of small molecules in selective and reversible manner, Chem. Mater. 27 (15) (2015) 5349–5360, https://doi.org/10.1021/acs.chemmater.5b01773.

[96] T. Gong, P. Li, Q. Sui, J. Chen, J. Xu, E.-Q. Gao, A stable electron-deficient metal–organic framework for colorimetric and luminescence sensing of phenols and anilines, J. Mater. Chem. A 6 (19) (2018) 9236–9244, https://doi.org/10.1039/C8TA02794C.

[97] C. He, K. Lu, W. Lin, Nanoscale metal–organic frameworks for real-time intracellular pH sensing in live cells, J. Am. Chem. Soc. 136 (35) (2014) 12253–12256, https://doi.org/10.1021/ja507333c.

[98] M. Pamei, A. Puzari, Luminescent transition metal–organic frameworks: an emerging sensor for detecting biologically essential metal ions, Nano-Struct. Nano-Objects 19 (2019) 100364, https://doi.org/10.1016/j.nanoso.2019.100364.

[99] S.A.A. Razavi, A. Morsali, Metal ion detection using luminescent-MOFs: Principles, strategies and roadmap, Coordinat. Chem. Rev. 415 (2020) 213299, https://doi.org/10.1016/j.ccr.2020.213299.

[100] A. Lan, K. Li, H. Wu, D. Olson, T. Emge, W. Ki, M. Hong, J. Li, A luminescent microporous metal-organic framework for the fast and reversible detection of high explosives, Angew. Chem. Int. Ed. 48 (13) (2009) 2334–2338, https://doi.org/10.1002/anie.200804853.

[101] Y. Zhang, B. Li, H. Ma, L. Zhang, W. Zhang, An RGH–MOF as a naked eye colorimetric fluorescent sensor for picric acid recognition, J. Mater. Chem. C 5 (19) (2017) 4661–4669, https://doi.org/10.1039/C7TC00936D.

[102] W.-J. Li, M. Tu, R. Cao, R.A. Fischer, Metal–organic framework thin films: electrochemical fabrication techniques and corresponding applications & perspectives, J. Mater. Chem. A. 4 (2016) 12356–12369, https://doi.org/10.1039/C6TA02118B.

[103] M. Li, M. Dincă, On the mechanism of MOF-5 formation under Cathodic Bias, Chem. Mater. 27 (9) (2015) 3203–3206, https://doi.org/10.1021/acs.chemmater.5b00899.

[104] F. Zhang, Y. Wang, T. Chu, Z. Wang, W. Li, Y. Yang, A facile fabrication of electrodeposited luminescent MOF thin films for selective and recyclable sensing of nitroaromatic explosives, Analyst 141 (14) (2016) 4502–4510, https://doi.org/10.1039/C6AN00840B.

[105] F. Zhang, G. Zhang, H. Yao, Y. Wang, T. Chu, Y. Yang, A europium (III) based nano-flake MOF film for efficient fluorescent sensing of picric acid, Microchim. Acta 184 (4) (2017) 1207–1213, https://doi.org/10.1007/s00604-017-2127-1.

[106] X. Zheng, C. Sun, S. Lu, F. Liao, S. Gao, L. Jin, New porous lanthanide-organic frameworks: synthesis, characterization, and properties of lanthanide 2,6-naphthalenedicarboxylates, Eur. J. Inorg. Chem. 2004 (16) (2004) 3262–3268, https://doi.org/10.1002/ejic.200400176.

[107] C.-H. Chen, X.-S. Wang, L. Li, Y.-B. Huang, R. Cao, Highly selective sensing of $Fe^{3+}$ by an anionic metal–organic framework containing uncoordinated nitrogen and carboxylate oxygen sites, Dalton Trans. 47 (10) (2018) 3452–3458, https://doi.org/10.1039/C8DT00088C.

[108] B. Wang, Q. Yang, C. Guo, Y. Sun, L.-H. Xie, J.-R. Li, Stable Zr(IV)-based metal–organic frameworks with predesigned functionalized ligands for highly selective detection of Fe(III) ions in water, ACS Appl. Mater. Interfaces 9 (11) (2017) 10286–10295, https://doi.org/10.1021/acsami.7b00918.

[109] C. Qiao, X. Qu, Q. Yang, Q. Wei, G. Xie, S. Chen, D. Yang, Instant high-selectivity Cd-MOF chemosensor for naked-eye detection of Cu(II) confirmed using in situ microcalorimetry, Green Chem. 18 (2016) 951–956, https://doi.org/10.1039/C5GC02393A.

[110] J. Zhang, J. Ouyang, Y. Ye, Z. Li, Q. Lin, T. Chen, Z. Zhang, S. Xiang, Mixed-valence cobalt(II/III) metal–organic framework for ammonia sensing with naked-eye color switching, ACS Appl. Mater. Interfaces 10 (32) (2018) 27465–27471, https://doi.org/10.1021/acsami.8b07770.

[111] B.-H. Liu, D.-X. Liu, K.-Q. Yang, S.-J. Dong, W. Li, Y.-J. Wang, A new cluster-based metal-organic framework with triazine backbones for selective luminescent detection of mercury(II) ion, Inorgan. Chem. Commun. 90 (2018) 61–64, https://doi.org/10.1016/j.inoche.2018.02.008.

[112] G.-S. Yang, Z.-L. Lang, H.-Y. Zang, Y.-Q. Lan, W.-W. He, X.-L. Zhao, L.-K. Yan, X.-L. Wang, Z.-M. Su, Control of interpenetration in S-containing metal–organic frameworks for selective separation of transition metal ions, Chem. Commun. 49 (11) (2013) 1088, https://doi.org/10.1039/c2cc36894c.

[113] Y. Zhao, X. Xu, L. Qiu, X. Kang, L. Wen, B. Zhang, Metal–organic frameworks constructed from a new thiophene-functionalized dicarboxylate: luminescence sensing and pesticide removal, ACS Appl. Mater. Interfaces 9 (17) (2017) 15164–15175, https://doi.org/10.1021/acsami.6b11797.

[114] W. Wu, B. Li, C. Gu, J. Wang, A. Singh, A. Kumar, Luminescent sensing of $Cu^{2+}$, $CrO_4^{2-}$ and photocatalytic degradation of methyl violet by Zn(II) metal-organic framework (MOF) having 5,5′-(1H–2,3,5-triazole-1,4-diyl) diisophthalic acid ligand, J. Mol. Struct. 1148 (2017) 531–536, https://doi.org/10.1016/j.mAolstruc.2017.07.083.
[115] A. Zhitkovich, Importance of chromium-DNA adducts in mutagenicity and toxicity of chromium(VI), Chem. Res. Toxicol. 18 (2005) 3–11, https://doi.org/10.1021/tx049774+.
[116] T. He, Y.-Z. Zhang, X.-J. Kong, J. Yu, X.-L. Lv, Y. Wu, Z.-J. Guo, J.-R. Li, Zr(IV)-Based metal-organic framework with T-shaped ligand: unique structure, high stability, selective detection, and rapid adsorption of $Cr_2O_7^{2-}$ in Water, ACS Appl. Mater. Interfaces 10 (19) (2018) 16650–16659, https://doi.org/10.1021/acsami.8b03987.
[117] S. Mohapatra, S. Adhikari, H. Riju, T.K. Maji, Terbium(III), Europium(III), and mixed terbium(III)–Europium(III) mucicate frameworks: hydrophilicity and stoichiometry-dependent color tunability, Inorg. Chem. 51 (9) (2012) 4891–4893, https://doi.org/10.1021/ic300237e.
[118] J.F.S. do Nascimento, A.M.U. de Araújo, J. Kulesza, A.F. de Farias Monteiro, S.A. Júnior, Bráulio.S. Barros, Solid-state tunable photoluminescence in gadolinium-organic frameworks: effects of the $Eu^{3+}$ content and co-doping with $Eu^{3+}$, New J. Chem. 42 (7) (2018) 5514–5522, https://doi.org/10.1039/C7NJ04625A.
[119] H. He, F. Sun, T. Borjigin, N. Zhao, G. Zhu, Tunable colors and white-light emission based on a microporous luminescent Zn(II)-MOF, Dalt. Trans. 43 (2014) 3716–3721, https://doi.org/10.1039/C3DT53013B.
[120] Y. Gai, Q. Guo, K. Xiong, F. Jiang, C. Li, X. Li, Y. Chen, C. Zhu, Q. Huang, R. Yao, M. Hong, Mixed-lanthanide metal–organic frameworks with tunable color and white light emission, Crystal Growth Design 17 (3) (2017) 940–944, https://doi.org/10.1021/acs.cgd.6b01541.
[121] X. Mi, D. Sheng, Y. Yu, Y. Wang, L. Zhao, J. Lu, Y. Li, D. Li, J. Dou, J. Duan, S. Wang, Tunable light emission and multiresponsive luminescent sensitivities in aqueous solutions of two series of lanthanide metal–organic frameworks based on structurally related ligands, ACS Appl. Mater. Interfaces 11 (8) (2019) 7914–7926, https://doi.org/10.1021/acsami.8b18320.
[122] Y. Yu, J.-P. Ma, Y.-B. Dong, Luminescent humidity sensors based on porous $Ln^{3+}$-MOFs, CrystEngComm 14 (21) (2012) 7157, https://doi.org/10.1039/c2ce26210j.
[123] L.K. Cadman, M.F. Mahon, A.D. Burrows, The effect of metal distribution on the luminescence properties of mixed-lanthanide metal–organic frameworks, Dalton Trans. 47 (7) (2018) 2360–2367, https://doi.org/10.1039/C7DT04583B.
[124] Q. Tang, S. Liu, Y. Liu, D. He, J. Miao, X. Wang, Y. Ji, Z. Zheng, Color Tuning and white light emission via in situ doping of luminescent lanthanide metal–organic frameworks, Inorg. Chem. 53 (1) (2014) 289–293, https://doi.org/10.1021/ic402228g.
[125] J. Liu, W. Sun, Z. Liu, White-light emitting materials with tunable luminescence based on steady Eu(III) doping of Tb(III) metal–organic frameworks, RSC Adv. 6 (2016) 25689–25694, https://doi.org/10.1039/C6RA01931E.
[126] D.K. Singha, P. Majee, S.K. Mondal, P. Mahata, Visible detection of explosive nitroaromatics facilitated by a large stokes shift of luminescence using europium and terbium doped yttrium based MOFs, RSC Adv. 5 (123) (2015) 102076–102084, https://doi.org/10.1039/C5RA22599J.
[127] S. Zou, Q. Li, S. Du, Efficient and tunable multi-color and white light Ln-MOFs with high luminescence quantum yields, RSC Adv. 5 (44) (2015) 34936–34941, https://doi.org/10.1039/C5RA03710G.
[128] P.R. Matthes, C.J. Höller, M. Mai, J. Heck, S.J. Sedlmaier, S. Schmiechen, C. Feldmann, W. Schnick, K. Müller-Buschbaum, Luminescence tuning of MOFs *via* ligand to metal and metal to metal energy transfer by co-doping of $^2{}_\infty[Gd_2Cl_6(bipy)_3]\cdot 2bipy$ with europium and terbium, J. Mater. Chem. 22 (20) (2012) 10179, https://doi.org/10.1039/c2jm15571k.
[129] S. Wang, L. Shan, Y. Fan, J. Jia, J. Xu, L. Wang, Fabrication of Ln-MOFs with color-tunable photoluminescence and sensing for small molecules, J. Solid State Chem. 245 (2017) 132–137, https://doi.org/10.1016/j.jssc.2016.10.006.
[130] S. Wang, J. Xu, J. Wang, K.-Y. Wang, S. Dang, S. Song, D. Liu, C. Wang, Luminescence of samarium(III) bis-dithiocarbamate frameworks: codoped lanthanide emitters that cover visible and near-infrared domains, J. Mater. Chem. C. 5 (2017) 6620–6628, https://doi.org/10.1039/C7TC01844D.
[131] M. Martínez-Calvo, O. Kotova, M.E. Möbius, A.P. Bell, T. McCabe, J.J. Boland, T. Gunnlaugsson, Healable luminescent self-assembly supramolecular metallogels possessing lanthanide (Eu/Tb) dependent rheological and morphological properties, J. Am. Chem. Soc. 137 (5) (2015) 1983–1992, https://doi.org/10.1021/ja511799n.
[132] V.K. Praveen, C. Ranjith, N. Armaroli, White-light-emitting supramolecular gels, Angew. Chem. Int. Ed. 53 (2) (2014) 365–368, https://doi.org/10.1002/anie.201306787.
[133] H. Kim, J. Young Chang, White light emission from a mixed organogel of lanthanide(iii)-containing organogelators, RSC Adv. 3 (2013) 1774–1780, https://doi.org/10.1039/c2ra22908k.
[134] Q.-Y. Yang, M. Pan, S.-C. Wei, K. Li, B.-B. Du, C.-Y. Su, Linear Dependence of photoluminescence in mixed Ln-MOFs for color tunability and barcode application, Inorg. Chem. 54 (12) (2015) 5707–5716, https://doi.org/10.1021/acs.inorgchem.5b00271.
[135] K.T. Kamtekar, A.P. Monkman, M.R. Bryce, Recent advances in white organic light-emitting materials and devices (WOLEDs), Adv. Mater. 22 (5) (2010) 572–582, https://doi.org/10.1002/adma.200902148.
[136] M. Shang, C. Li, J. Lin, How to produce white light in a single-phase host?, Chem Soc. Rev. 43 (5) (2014) 1372–1386, https://doi.org/10.1039/C3CS60314H.
[137] C.-H. Huang, W.-R. Liu, T.-M. Chen, Single-phased white-light phosphors $Ca_9Gd(PO_4)_7$:$Eu^{2+}$, $Mn^{2+}$ under Near-ultraviolet excitation, J. Phys. Chem. C 114 (43) (2010) 18698–18701, https://doi.org/10.1021/jp106693z.
[138] J. Qiao, J. Zhao, Q. Liu, Z. Xia, Recent advances in solid-state LED phosphors with thermally stable luminescence, J. Rare Earths 37 (6) (2019) 565–572, https://doi.org/10.1016/j.jre.2018.11.001.
[139] J. Cornelio, T.-Y. Zhou, A. Alkaş, S.G. Telfer, Systematic tuning of the luminescence output of multicomponent metal–organic frameworks, J. Am. Chem. Soc. 140 (45) (2018) 15470–15476, https://doi.org/10.1021/jacs.8b09887.
[140] Y. Cui, T. Song, J. Yu, Y. Yang, Z. Wang, G. Qian, Dye encapsulated metal-organic framework for warm-white LED with high color-rendering index, Adv. Funct. Mater. 25 (30) (2015) 4796–4802, https://doi.org/10.1002/adfm.201501756.
[141] J. Yu, Y. Cui, C. Wu, Y. Yang, Z. Wang, M. O'Keeffe, B. Chen, G. Qian, Second-order nonlinear optical activity induced by ordered dipolar chromophores confined in the pores of an anionic metal-organic framework, Angew. Chem. Int. Ed. 51 (42) (2012) 10542–10545, https://doi.org/10.1002/anie.201204160.
[142] S.R. Forrest, The road to high efficiency organic light emitting devices, Org. Electron. 4 (2-3) (2003) 45–48, https://doi.org/10.1016/j.orgel.2003.08.014.
[143] M. Aleksandrova, Specifics and challenges to flexible organic light-emitting devices, Adv. Mater. Sci. Eng. 2016 (2016) 1–8, https://doi.org/10.1155/2016/4081697.
[144] M. Gutiérrez, C. Martin, K. Kennes, J. Hofkens, M. Van der Auweraer, Félix Sánchez, A. Douhal, New OLEDs Based on zirconium metal-organic framework, Adv. Opt. Materials 6 (6) (2018) 1–12, https://doi.org/10.1002/adom.201701060.
[145] F.W. Steuber, J.J. Gough, Éadaoin Whelan, L. Burtnyak, A.L. Bradley, W. Schmitt, Node-dependent photoinduced electron transfer in third-generation 2D MOFs containing earth-abundant metal ions, Inorg. Chem. 59 (23) (2020) 17244–17250, https://doi.org/10.1021/acs.inorgchem.0c02475.
[146] A.S. Agarwal, E. Rode, N. Sridhar, D. Hill, Conversion of CO2 to Value Added Chemicals: Opportunities and Challenges, in: W.-Y. Chen, T. Suzuki, M. Lackner (Eds.), Handbook of Climate Change Mitigation and Adaptation, Springer International Publishing, Cham, 2016: pp. 2487–2526. Doi: 10.1007/978-3-319-14409-2_86.
[147] J. Kothandaraman, A. Goeppert, M. Czaun, G.A. Olah, G.K.S. Prakash, Conversion of $CO_2$ from air into methanol using a polyamine and a homogeneous ruthenium catalyst, J. Am. Chem. Soc. 138 (3) (2016) 778–781, https://doi.org/10.1021/jacs.5b12354.
[148] A. Kidanemariam, J. Lee, J. Park, Recent innovation of metal-organic frameworks for carbon dioxide photocatalytic reduction, Polymers (Basel). 11 (2019) 2090. Doi: 10.3390/polym11122090.
[149] I.I. Alkhatib, C. Garlisi, M. Pagliaro, K. Al-Ali, G. Palmisano, Metal-organic frameworks for photocatalytic $CO_2$ reduction under visible radiation: a review of strategies and applications, Catal. Today 340 (2020) 209–224, https://doi.org/10.1016/j.cattod.2018.09.032.
[150] A. Fujishima, K. Honda, Electrochemical photolysis of water at a semiconductor electrode, Nature 238 (5358) (1972) 37–38, https://doi.org/10.1038/238037a0.
[151] A.J. Morris, G.J. Meyer, E. Fujita, Molecular approaches to the photocatalytic reduction of carbon dioxide for solar fuels, Acc. Chem. Res. 42 (12) (2009) 1983–1994, https://doi.org/10.1021/ar9001679.
[152] C.S. Diercks, Y. Liu, K.E. Cordova, O.M. Yaghi, The role of reticular chemistry in the design of $CO_2$ reduction catalysts, Nature Mater 17 (4) (2018) 301–307, https://doi.org/10.1038/s41563-018-0033-5.
[153] C. Wang, Z. Xie, K.E. deKrafft, W. Lin, Doping metal–organic frameworks for water oxidation, carbon dioxide reduction, and organic photocatalysis, J. Am. Chem. Soc. 133 (34) (2011) 13445–13454, https://doi.org/10.1021/ja203564w.
[154] J.H. Cavka, S. Jakobsen, U. Olsbye, N. Guillou, S. Bordiga, K.P. Lillerud, C. Lamberti, S. Bordiga, K.P. Lillerud, A new zirconium inorganic building brick forming metal organic frameworks with exceptional stability, J. Am. Chem. Soc. 130 (2008) 1–19, https://doi.org/10.1021/ja8057953.
[155] K.A. Vincent, G.J. Tilley, N.C. Quammie, I. Streeter, B.K. Burgess, M.R. Cheesman, F.A. Armstrong, Instantaneous, stoichiometric generation of powerfully reducing states of protein active sites using Eu(ii) and polyaminocarboxylate ligands, Chem. Commun. (20) (2003) 2590, https://doi.org/10.1039/b308188e.
[156] C.C. Lee, Y. Hu, M.W. Ribbe, ATP-independent substrate reduction by nitrogenase P-cluster variant, Proceed. Natl. Acad. Sci. 109 (18) (2012) 6922–6926, https://doi.org/10.1073/pnas.1202429109.
[157] S. Zhang, L. Li, S. Zhao, Z. Sun, J. Luo, Construction of interpenetrated ruthenium metal–organic frameworks as stable photocatalysts for $CO_2$ reduction, Inorg. Chem. 54 (17) (2015) 8375–8379, https://doi.org/10.1021/acs.inorgchem.5b01045.
[158] C.J. Setter, M.B. Price, L. Conte, W. Schmitt, S.R. Batten, C. Richardson, M.R. Hill, R. Babarao, L.K. Macreadie, Mixed donor, phenanthroline photoactive MOFs with favourable $CO_2$ selectivity, Chem. Commun. 56 (87) (2020) 13377–13380, https://doi.org/10.1039/D0CC05715K.
[159] D. Wang, R. Huang, W. Liu, D. Sun, Z. Li, Fe-based MOFs for photocatalytic $CO_2$ reduction: role of coordination unsaturated sites and dual excitation

pathways, ACS Catal. 4 (12) (2014) 4254–4260, https://doi.org/10.1021/cs501169t.
[160] S. Bauer, C. Serre, T. Devic, P. Horcajada, J. Marrot, G. Férey, N. Stock, High-throughput assisted rationalization of the formation of metal organic frameworks in the Iron(III) aminoterephthalate solvothermal system, Inorg. Chem. 47 (17) (2008) 7568–7576, https://doi.org/10.1021/ic800538r.
[161] P. Horcajada, F. Salles, S. Wuttke, T. Devic, D. Heurtaux, G. Maurin, A. Vimont, M. Daturi, O. David, E. Magnier, N. Stock, Y. Filinchuk, D. Popov, C. Riekel, Gérard Férey, C. Serre, How linker's modification controls swelling properties of highly flexible iron(III) dicarboxylates MIL-88, J. Am. Chem. Soc. 133 (44) (2011) 17839–17847, https://doi.org/10.1021/ja206936e.
[162] O.I. Lebedev, F. Millange, C. Serre, G. Van Tendeloo, G. Férey, First direct imaging of giant pores of the metal–organic framework MIL-101, Chem. Mater. 17 (26) (2005) 6525–6527, https://doi.org/10.1021/cm051870o.
[163] M. Dan-Hardi, C. Serre, T. Frot, L. Rozes, G. Maurin, C. Sanchez, G. Férey, A new photoactive crystalline highly porous titanium(IV) dicarboxylate, J. Am. Chem. Soc. 131 (31) (2009) 10857–10859, https://doi.org/10.1021/ja903726m.
[164] Y. Fu, D. Sun, Y. Chen, R. Huang, Z. Ding, X. Fu, Z. Li, An amine-functionalized titanium metal-organic framework photocatalyst with visible-light-induced activity for $CO_2$ reduction, Angew. Chem. Int. Ed. 51 (14) (2012) 3364–3367, https://doi.org/10.1002/anie.201108357.
[165] M. Liu, Y.-F. Mu, S. Yao, S. Guo, X.-W. Guo, Z.-M. Zhang, T.-B. Lu, Photosensitizing single-site metal–organic framework enabling visible-light-driven $CO_2$ reduction for syngas production, Appl. Catal. B: Environ. 245 (2019) 496–501, https://doi.org/10.1016/j.apcatb.2019.01.014.
[166] K. Aasberg-Petersen, I. Dybkjær, C.V. Ovesen, N.C. Schjødt, J. Sehested, S.G. Thomsen, Natural gas to synthesis gas – Catalysts and catalytic processes, J. Nat. Gas Sci. Eng. 3 (2) (2011) 423–459, https://doi.org/10.1016/j.jngse.2011.03.004.
[167] J.H. Kim, D. Hansora, P. Sharma, J.-W. Jang, J.S. Lee, Toward practical solar hydrogen production – an artificial photosynthetic leaf-to-farm challenge, Chem. Soc. Rev. 48 (7) (2019) 1908–1971, https://doi.org/10.1039/C8CS00699G.
[168] H. Ahmad, S.K. Kamarudin, L.J. Minggu, M. Kassim, Hydrogen from photocatalytic water splitting process: a review, Renew. Sustain. Energy Rev. 43 (2015) 599–610, https://doi.org/10.1016/j.rser.2014.10.101.
[169] E.M. Sproviero, J.A. Gascón, J.P. Mcevoy, G.W. Brudvig, V.S. Batista, Computational studies of the $O_2$-evolving complex of photosystem II and biomimetic oxomanganese complexes, Coord. Chem. Rev. 252 (3-4) (2008) 395–415, https://doi.org/10.1016/j.ccr.2007.09.006.
[170] Y. Kato, F. Akita, Y. Nakajima, M. Suga, Y. Umena, J.-R. Shen, T. Noguchi, Fourier transform infrared analysis of the S-state cycle of water oxidation in the microcrystals of photosystem II, J. Phys. Chem. Lett. 9 (9) (2018) 2121–2126, https://doi.org/10.1021/acs.jpclett.8b00638.
[171] M. Suga, F. Akita, K. Hirata, G. Ueno, H. Murakami, Y. Nakajima, T. Shimizu, K. Yamashita, M. Yamamoto, H. Ago, J.R. Shen, Native structure of photosystem II at 1.95Å resolution viewed by femtosecond X-ray pulses, Nature 517 (2015) 99–103, https://doi.org/10.1038/nature13991.
[172] Y. Umena, K. Kawakami, J.R. Shen, N. Kamiya, Crystal structure of oxygen-evolving photosystem II at a resolution of 1.9Å, Nature. 473 (2011) 55–60, https://doi.org/10.1038/nature09913.
[173] B. Kok, B. Forbush, M. Mcgloin, Cooperation of charges in photosynthetic $O_2$ evolution–I. A linear four step mechanism, Photochem. Photobiol. 11 (6) (1970) 457–475, https://doi.org/10.1111/j.1751-1097.1970.tb06017.x.
[174] E.M. Miner, M. Dincă, Metal-organic frameworks: Evolved oxygen evolution catalysts, Nat. Energy 1 (12) (2016), https://doi.org/10.1038/nenergy.2016.186.
[175] Ülkü Kökçam-Demir, A. Goldman, L. Esrafili, M. Gharib, A. Morsali, O. Weingart, C. Janiak, Coordinatively unsaturated metal sites (open metal sites) in metal–organic frameworks: design and applications, Chem. Soc. Rev. 49 (9) (2020) 2751–2798, https://doi.org/10.1039/C9CS00609E.
[176] N.-Y. Huang, J.-Q. Shen, Z.-M. Ye, W.-X. Zhang, P.-Q. Liao, X.-M. Chen, An exceptionally stable octacobalt-cluster-based metal–organic framework for enhanced water oxidation catalysis, Chem. Sci. 10 (42) (2019) 9859–9864, https://doi.org/10.1039/C9SC03224J.
[177] G. Lan, Y.-Y. Zhu, S.S. Veroneau, Z. Xu, D. Micheroni, W. Lin, Electron injection from photoexcited metal–organic framework ligands to $Ru_2$ secondary building units for visible-light-driven hydrogen evolution, J. Am. Chem. Soc. 140 (16) (2018) 5326–5329, https://doi.org/10.1021/jacs.8b01601.
[178] W.A. Shah, A. Waseem, M.A. Nadeem, P. Kögerler, Leaching-free encapsulation of cobalt-polyoxotungstates in MIL-100 (Fe) for highly reproducible photocatalytic water oxidation, Appl. Catal. A: Gen. 567 (2018) 132–138, https://doi.org/10.1016/j.apcata.2018.08.002.
[179] P. Horcajada, S. Surblé, C. Serre, D.-Y. Hong, Y.-K. Seo, J.-S. Chang, J.-M. Grenèche, I. Margiolaki, G. Férey, Synthesis and catalytic properties of MIL-100(Fe), an iron(III) carboxylate with large pores, Chem. Commun. 100 (2007) 2820–2822, https://doi.org/10.1039/B704325B.
[180] F. Song, Y. Ding, B. Ma, C. Wang, Q. Wang, X. Du, S. Fu, J. Song, $K_7[Co^{III}Co^{II}(H_2O)W_{11}O_{39}]$: a molecular mixed-valence Keggin polyoxometalate catalyst of high stability and efficiency for visible light-driven water oxidation, Energy Environ. Sci. 6 (4) (2013) 1170, https://doi.org/10.1039/c3ee24433d.
[181] Q. Yin, J.M. Tan, C. Besson, Y.V. Geletii, D.G. Musaev, A.E. Kuznetsov, Z. Luo, K.I. Hardcastle, C.L. Hill, A fast soluble carbon-free molecular water oxidation catalyst based on abundant metals, Science 328 (5976) (2010) 342–345, https://doi.org/10.1126/science.1185372.
[182] Z.-M. Zhang, T. Zhang, C. Wang, Z. Lin, L.-S. Long, W. Lin, Photosensitizing metal–organic framework enabling visible-light-driven proton reduction by a Wells–Dawson-type polyoxometalate, J. Am. Chem. Soc. 137 (9) (2015) 3197–3200, https://doi.org/10.1021/jacs.5b00075.
[183] D. Shi, R. Zheng, M.-J. Sun, X. Cao, C.-X. Sun, C.-J. Cui, C.-S. Liu, J. Zhao, M. Du, Semiconductive copper(I)-organic frameworks for efficient light-driven hydrogen generation without additional photosensitizers and cocatalysts, Angew. Chem. Int. Ed. 56 (46) (2017) 14637–14641, https://doi.org/10.1002/anie.201709869.
[184] O.M. Yaghi, G. Li, Mutually interpenetrating sheets and channels in the extended structure of[Cu(4,4′-bpy)Cl], Angew. Chem. Int. Ed. Engl. 34 (2) (1995) 207–209, https://doi.org/10.1002/anie.199502071.
[185] S.R. Batten, J.C. Jeffery, M.D. Ward, Studies of the construction of coordination polymers using linear pyridyl-donor ligands, Inorgan. Chim. Acta 292 (2) (1999) 231–237, https://doi.org/10.1016/S0020-1693(99)00203-0.
[186] D.A. Yaseen, M. Scholz, Textile dye wastewater characteristics and constituents of synthetic effluents: a critical review, Int. J. Environ. Sci. Technol. 16 (2) (2019) 1193–1226, https://doi.org/10.1007/s13762-018-2130-z.
[187] B. Lellis, Cíntia.Z. Fávaro-Polonio, João.A. Pamphile, J.C. Polonio, Effects of textile dyes on health and the environment and bioremediation potential of living organisms, Biotechnol. Res. Innovat. 3 (2) (2019) 275–290, https://doi.org/10.1016/j.biori.2019.09.001.
[188] Y. Pan, Q. Ding, H. Xu, C. Shi, A. Singh, A. Kumar, J. Liu, A new Zn(II)-based 3D metal–organic framework with uncommon **sev** topology and its photocatalytic properties for the degradation of organic dyes, CrystEngComm. 21 (2019) 4578–4585, https://doi.org/10.1039/C9CE00759H.
[189] Y. Gao, S. Li, Y. Li, L. Yao, H. Zhang, Accelerated photocatalytic degradation of organic pollutant over metal-organic framework MIL-53(Fe) under visible LED light mediated by persulfate, Appl. Catal. B: Environ. 202 (2017) 165–174, https://doi.org/10.1016/j.apcatb.2016.09.005.
[190] Y. Zhou, W. Yang, M. Qin, H. Zhao, Self-assembly of metal-organic framework thin films containing metalloporphyrin and their photocatalytic activity under visible light: Visible-light photocatalytic activity of MnPor-MOF thin-film, Appl. Organometal. Chem. 30 (4) (2016) 188–192, https://doi.org/10.1002/aoc.3415.
[191] M.Jesús. García-Galán, T. Garrido, J. Fraile, A. Ginebreda, M.S. Díaz-Cruz, D. Barceló, Simultaneous occurrence of nitrates and sulfonamide antibiotics in two ground water bodies of Catalonia (Spain), J. Hydrol. 383 (1-2) (2010) 93–101, https://doi.org/10.1016/j.jhydrol.2009.06.042.
[192] B. Aslam, W. Wang, M.I. Arshad, M. Khurshid, S. Muzammil, M.H. Rasool, M.A. Nisar, R.F. Alvi, M.A. Aslam, M.U. Qamar, M.K.F. Salamat, Z. Baloch, Antibiotic resistance: a rundown of a global crisis, Infect. Drug Resist. 11 (2018) 1645–1658, https://doi.org/10.2147/IDR.S173867.
[193] X. Liu, B. Liu, G. Li, Y. Liu, Two anthracene-based metal–organic frameworks for highly effective photodegradation and luminescent detection in water, J. Mater. Chem. A 6 (35) (2018) 17177–17185, https://doi.org/10.1039/C8TA03807D.
[194] Li Minyuan, Dincă Mircea, Reductive Electrosynthesis of Crystalline Metal–Organic Frameworks, Journal of the American Chemical Society 133 (33) (2011) 12926–12929, https://doi.org/10.1021/ja2041546.